

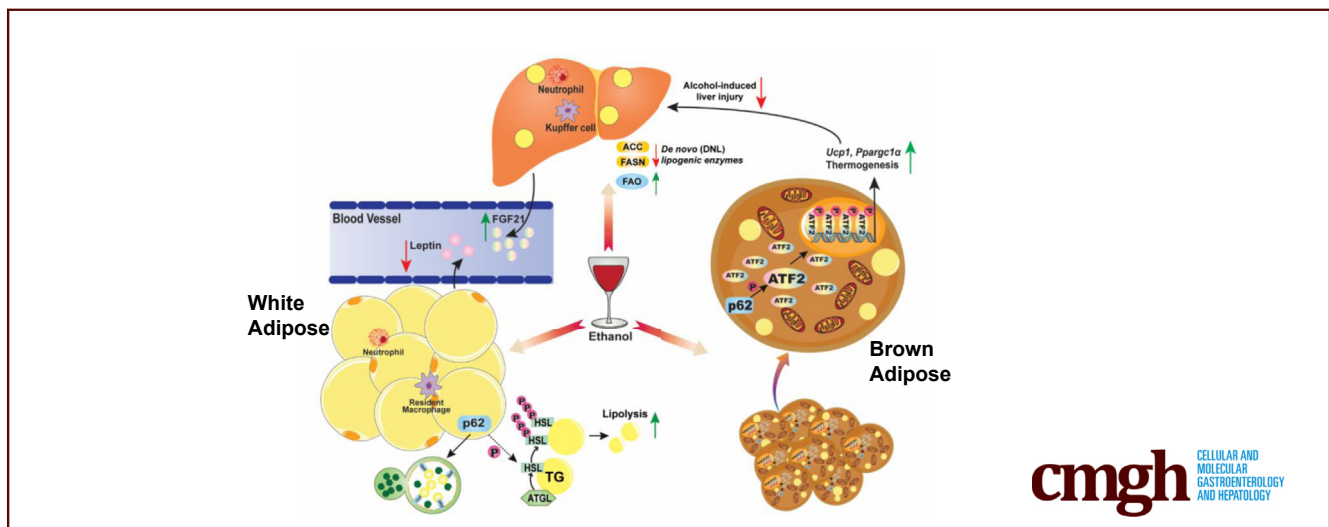
## ORIGINAL RESEARCH

## Loss of SQSTM1/p62 Induces Obesity and Exacerbates Alcohol-Induced Liver Injury in Aged Mice



Hui Qian,<sup>1</sup> Xiaojuan Chao,<sup>1</sup> Shaogui Wang,<sup>1</sup> Yuan Li,<sup>1</sup> Xiaoxiao Jiang,<sup>1</sup> Zhaoli Sun,<sup>2</sup> Thomas Rüllicke,<sup>3</sup> Kurt Zatloukal,<sup>4</sup> Hong-Min Ni,<sup>1</sup> and Wen-Xing Ding<sup>1,5</sup>

<sup>1</sup>Department of Pharmacology, Toxicology and Therapeutics, University of Kansas Medical Center, Kansas City, Kansas; <sup>2</sup>Department of Surgery, Johns Hopkins School of Medicine, Baltimore, Maryland; <sup>3</sup>Department of Biomedical Sciences, University of Veterinary Medicine Vienna, Vienna, Austria; <sup>4</sup>Institute of Pathology, Medical University of Graz, Graz, Austria; and <sup>5</sup>Department of Internal Medicine, University of Kansas Medical Center, Kansas City, Kansas



## SUMMARY

Loss of SQSTM1/p62 leads to adipose tissue dysfunction and mature-onset obesity in mice. Loss of SQSTM1/p62 leads to brown adipose tissue maladaptation to alcohol consumption resulting in more severe liver injury.

**BACKGROUND:** Alcohol-associated liver disease (ALD) is a worldwide health problem, of which the effective treatment is still lacking. Both detrimental and protective roles of adipose tissue have been implicated in ALD. Although alcohol increases adipose tissue lipolysis to promote alcohol-induced liver injury, alcohol also activates brown adipose tissue (BAT) thermogenesis as an adaptive response in protecting against alcohol-induced liver injury. Moreover, aging and obesity are also risk factors for ALD. In the present study, we investigated the effects of autophagy receptor protein SQSTM1/p62 on adipose tissue and obesity in alcohol-induced liver injury in both young and aged mice.

**METHODS:** Young and aged whole-body SQSTM1/p62 knockout (KO) and their age-matched wild-type (WT)

mice were subjected to chronic plus binge (Gao-binge) alcohol feeding. Blood, adipose and liver tissues were collected for biochemical and histologic analysis.

**RESULTS:** Aged but not young SQSTM1/p62 KO mice had significantly increased body weight and fat mass compared with the matched WT mice. Gao-binge alcohol feeding induced white adipose atrophy and decreased levels of SQSTM1/p62 levels in adipose tissue in aged WT mice. SQSTM1/p62 KO aged mice were resistant to Gao-binge alcohol-induced white adipose atrophy. Alcohol feeding increased the expression of thermogenic genes in WT mouse BAT, which was significantly blunted in SQSTM1/p62 KO aged mice. Alcohol-fed aged SQSTM1/p62 KO mice showed significantly higher levels of serum alanine aminotransferase, hepatic triglyceride, and inflammation compared with young and aged WT mice fed with alcohol. Alcohol-fed SQSTM1/p62 KO mice also increased secretion of proinflammatory and angiogenic adipokines that may promote alcohol-induced liver injury.

**CONCLUSIONS:** Loss of SQSTM1/p62 in aged mice leads to obesity and impairs alcohol-induced BAT adaptation, resulting in exacerbated alcohol-induced liver injury in mice. (*Cell Mol*

*Gastroenterol Hepatol* 2023;15:1027-1049; <https://doi.org/10.1016/j.jcmgh.2023.01.016>

**Keywords:** Adipose Tissue; Adipokine; ALD; Autophagy; Steatosis.


Alcohol-associated liver disease (ALD) is a major form of chronic liver disease that claims 2 million lives each year worldwide.<sup>1</sup> ALD is also the most common cause of non-malignant gastrointestinal diseases in the United States.<sup>2,3</sup> The pathogenesis of ALD is characterized by 5 major stages: steatosis, steatohepatitis, fibrosis, cirrhosis, and hepatocellular carcinoma (HCC).<sup>4-6</sup> Steatosis refers to excess lipid droplets (LD) accumulation in hepatocytes, whereas alcoholic steatohepatitis (AH) is characterized by the presence of inflammation and hepatocyte injury such as ballooning, formation of Mallory-Denk bodies (MDB), and cell death in the liver. If prolonged, AH can further progress to cirrhosis, in which the liver becomes irreversibly scarred and liver failure occurs.<sup>7</sup> Notably, alcohol-related liver cirrhosis is becoming a leading cause of elevated mortality and morbidity worldwide.<sup>8,9</sup> Moreover, there is no Food and Drug Administration approved drug for ALD treatment. Currently, the most effective treatment for ALD is alcohol abstinence, and the only option for patients with advanced alcohol-related cirrhosis is liver transplantation.<sup>10,11</sup> Thus, it is urgently needed to better understand the pathologic mechanisms of ALD, which may help to identify potential therapeutic targets for treating ALD and supporting effects of lifestyle changes.

As the aging population grows dramatically and becomes a new global issue,<sup>12,13</sup> the prevalence of ALD in the elderly population is also increasing.<sup>14-16</sup> A wide variety of factors associated with aging such as increased hepatic infiltration of inflammatory cells,<sup>17,18</sup> decreased alcohol metabolism,<sup>19</sup> and reduced liver regeneration<sup>20</sup> can aggravate ALD in elderly people. Both ALD and aging are associated with dysregulated autophagy, and compromised autophagy is a hallmark of aging.<sup>21-23</sup> Autophagy, a cellular self-degradation mechanism, is important not only for maintaining hepatocyte homeostasis but also for reducing alcohol-induced hepatic steatosis and liver injury.<sup>24-26</sup> Autophagy activity decreases in an age-dependent manner,<sup>27-29</sup> leading to lipid accumulation and glucose homeostasis alteration in the liver.<sup>30-32</sup> Lysosome-associated membrane protein type 2A (LAMP-2A) is a key regulator of chaperone-mediated autophagy. LAMP-2A decreases in aged mouse liver, leading to the accumulation of hepatic-oxidized damaged proteins and liver injury, which can be improved by restoring hepatic LAMP-2A.<sup>33,34</sup> Previous studies from others and our lab show that alcohol consumption suppresses hepatic autophagy by inhibiting transcription factor EB (TFEB)-mediated lysosomal biogenesis, resulting in the accumulation of megamitochondria, LDs, and proteins.<sup>24,35-37</sup> Sequestosome 1 (SQSTM1/p62) (hereafter referred to as p62) is an autophagy substrate and receptor protein, and impaired autophagy leads to accumulation of p62. Increased intracellular p62 can form large protein aggregates/inclusions and is also a main component

of MDB found in ALD.<sup>38-40</sup> In addition to protein aggregates, p62 also acts as an intracellular signaling hub and involves in multiple signaling pathways including nuclear factor erythroid 2-related factor 2 (Nrf2), nuclear factor kappa B (NF $\kappa$ B), and the mammalian target of rapamycin (mTOR), which are critical for oxidative stress, inflammation, cell survival, metabolism, and liver tumorigenesis.<sup>41-44</sup>

Mice and humans have 3 different types of adipose tissue: white adipose tissue (WAT), brown adipose tissue (BAT), and beige adipose tissue. The main function of WAT is to store extra energy as triglycerides (TG), whereas BAT and beige adipocytes oxidize free fatty acids (FFAs) to generate heat to maintain body temperature homeostasis. Alcohol affects the adipose-liver axis, which can either be detrimental or beneficial to alcohol-induced liver pathogenesis. On the one hand, alcohol consumption increases WAT lipolysis and induces adipose atrophy, which may contribute to ALD by altering the adipose-liver axis in experimental ALD models.<sup>45-47</sup> On the other hand, alcohol consumption activates BAT by up-regulating the expression of uncoupling protein 1 (Ucp1) likely via the hypothalamic neural circuits, sympathetic innervating BAT and bile acid-mediated Takeda G-protein-coupled bile acid receptor 5 (TGR5) activation, which acts as an adaptive response to protect against alcohol-induced liver injury.<sup>48,49</sup> Notably, Gao-binge alcohol decreases p62 in adipose and promotes adipose tissue atrophy in mice.<sup>47</sup> The p62 whole-body knockout (KO) or adipose-specific p62 KO mice develop severe mature-onset obesity due to impaired BAT functions and decreased energy expenditure.<sup>50-52</sup> Emerging evidence indicates that p62 has antiaging effects, and decreased p62 expression is associated with aging.<sup>53,54</sup> Hepatic mRNA

**Abbreviations used in this paper:** Acadl, acyl-coenzyme A dehydrogenase, long-chain; Acadm, acyl-coenzyme A dehydrogenase, medium chain; ACC $\alpha$ , acetyl-coA carboxylase  $\alpha$ ; Acox1, acyl-coenzyme A oxidase 1; Adgre1, adhesion G protein-coupled receptor E1; AH, alcoholic steatohepatitis; ALD, alcohol-associated liver disease; ALT, alanine aminotransferase; ATF2, activating transcription factor 2; BAT, brown adipose tissue; C/EBP, CCAAT/enhancer-binding protein; Ccl2, chemokine (C-C motif) ligand 2; CIDEA, cell death-inducing DNA fragmentation factor, alpha subunit-like effector A; CLS, crown-like structure; Cox8 $\beta$ , cytochrome c oxidase subunit 8B; Cpt1 $\alpha$ , carnitine palmitoyltransferase 1 $\alpha$ ; DIO2, deiodinase, iodothyronine, type II; ERK, mitogen-activated protein kinase; eWAT, epididymal white adipose tissue; FASN, fatty acid synthase; FFA, free fatty acid; FGF, fibroblast growth factor; HCC, hepatocellular carcinoma; HGF, hepatocyte growth factor; HSL, hormone-sensitive lipase; IL, interleukin; KO, knockout; LAMP-2A, lysosome-associated membrane protein type 2A; LD, lipid droplet; MDB, Mallory-Denk body; MPO, myeloperoxidase; mTOR, mammalian target of rapamycin; NF $\kappa$ B, nuclear factor kappa B; Nrf2, nuclear factor erythroid 2-related factor 2; PPAR, peroxisome proliferator-activated receptor; Ppargc-1 $\alpha$ , PPARG coactivator 1 alpha; PRDM16, PR domain containing 16; Pref-1, preadipocyte factor-1; RBP4, retinol-binding protein-4; SELE, selectin E; Serpin E1, plasminogen activator inhibitor-1 (PAI-1); SQSTM1/p62, sequestosome 1; TFEB, transcription factor EB; TG, triglycerides; TGR5, Takeda G-protein-coupled bile acid receptor 5; TIMP-1, tissue inhibitor of metalloproteinases-1; TOM20, translocase of the outer membrane 20; UCP1, uncoupling protein 1; VEGF, vascular endothelial growth factor; WAT, white adipose tissue; WT, wild-type.

 Most current article

© 2023 The Authors. Published by Elsevier Inc. on behalf of the AGA Institute. This is an open access article under the CC BY-NC-ND license (<http://creativecommons.org/licenses/by-nc-nd/4.0/>).

2352-345X

<https://doi.org/10.1016/j.jcmgh.2023.01.016>

levels of *Sqstm1* decreased significantly with aging in mouse livers, and hepatic *Sqstm1* is only 5% in 132-week-old mice compared with 12-week-old mice.<sup>54</sup> However, the role and mechanisms by which p62 and aging coordinately affect the pathogenesis of ALD are unclear.

In this study, we found that chronic plus binge alcohol (Gao-binge alcohol) feeding decreased adipose p62 but increased hepatic p62 aggregates in wild-type (WT) aged mice. Loss of p62 in aged mice led to obesity and BAT maladaptation in response to alcohol feeding that exacerbated alcohol-induced liver injury.

## Results

### *Hepatic p62 Expression and Aggregation Are Elevated in Patients With Alcoholic Hepatitis and in Aged Mice Fed With Gao-Binge Alcohol*

Results from Western blot analysis showed that the levels of hepatic p62 and LC3-II were significantly higher in AH patients compared with the healthy human donor (Figure 1A and B). p62 also displayed smear patterns in AH samples likely due to increased post-translational modifications or increased formation of p62 oligomerization/aggregation. H&E staining revealed increased numbers of hepatocyte ballooning (arrowheads), LD (solid black arrows), and MDB (empty arrow) (Figure 1C). Immunohistochemistry staining of p62 showed weak diffuse pattern in normal healthy control livers but displayed massive aggregate pattern (typical feature of MDB) in AH patients (Figure 1D, empty arrows). The levels of hepatic p62 and LC3-II decreased in Gao-binge alcohol-fed young mice (Figure 2A and B), which is consistent with previously reported “insufficient autophagic flux” induced by alcohol in mouse livers.<sup>35</sup> However, in Gao-binge alcohol-fed aged mice, the level of hepatic p62 did not change or even slightly increased, but the level of LC3-II was significantly increased, which is likely due to impaired autophagic degradation of p62 and LC3-II in alcohol-fed aged mice (Figure 2C and D). Results from the immunofluorescence staining showed increased p62 aggregates in alcohol-fed aged but not young mice (Figure 2E). In addition to promoting protein aggregates, p62 can undergo phase separation to form gel-like p62 bodies or condensates in cells.<sup>55,56</sup> We next determined the levels of p62 in the detergent (Triton X-100) insoluble fractions from young and aged WT mice with or without alcohol feeding. Interestingly, no significant differences for the levels of p62 in the insoluble fractions were found in either young or aged mice by Gao-binge alcohol feeding (Figure 2F and G). Taken together, these results indicate that human AH patient livers have increased hepatic p62 aggregates. Alcohol may increase hepatic p62 protein aggregates but not p62 condensates in aged mice.

### *The Impacts of Hepatic p62 on the Levels of Detergent Insoluble Ubiquitinated Proteins in Young and Aged Mice Fed With a Control Diet or Gao-Binge Alcohol*

We found that hepatic insoluble levels of ubiquitinated proteins were much lower in young p62 KO mice compared

with young WT mice after alcohol feeding (Figure 3A and B), suggesting p62 may be required for the formation of a portion of insoluble ubiquitinated protein aggregates or condensates in young mice fed with alcohol. Interestingly, the levels of insoluble ubiquitinated proteins were significantly higher in aged p62 KO mice fed with alcohol compared with aged WT mice fed with a control diet or alcohol (Figure 3C and D), suggesting ubiquitinated protein aggregates can be formed independent of p62 in aged mice. Similarly, aged p62 KO mice also had higher levels of ubiquitinated proteins compared with aged WT mice fed with a control diet (Figure 3E and F). No differences in the levels of insoluble ubiquitinated proteins were found between young and aged mice regardless of genotypes and alcohol, suggesting aging alone does not have a significant impact on the levels of ubiquitinated protein aggregates (Figure 3E–H). The levels of p62 in the insoluble fractions were also almost identical between young and aged mice regardless of genotypes and alcohol (Figure 3E–H). Taken together, p62 may be required for alcohol-induced formation of ubiquitinated protein aggregates in young mice but not aged mice.

### *Loss of p62 Induces Mature-Onset Obesity and Promotes Gao-Binge Alcohol-Induced Hepatic Steatosis and Liver Injury in Aged Mice*

Because we observed increased p62 accumulation in human AH livers and alcohol-fed aged mouse livers, we generated p62 KO mice and fed these mice with Gao-binge alcohol to further dissect the role of p62 in the pathogenesis of ALD. In young mice (3-month-old or 3M), there were no significant differences in terms of body weight, liver weight, and the ratio of liver to body weight, regardless of genotype and alcohol feeding. However, in aged mice (14-month-old or 14M) fed with control diet, except the ratio of liver to body weight, the body weight and liver weight in p62 KO mice were significantly higher than WT mice (Figure 4A–D), suggesting that loss of p62 leads to mature-onset obesity as previously reported.<sup>50</sup> Gao-binge alcohol feeding did not affect body weight, liver weight, or ratio of liver to body weight in aged WT mice. However, Gao-binge alcohol feeding further increased liver weight and ratio of liver to body weight in aged p62 KO mice (Figure 4A–D), suggesting that loss of p62 promotes liver weight gain in alcohol-fed aged mice. No difference in food consumption by measuring the volume of liquid diet consumed each day per mouse was observed between young WT and p62 KO mice. Although aged p62 KO mice had increased food intake, the food intake (both control and alcohol diet) in aged p62 KO and WT mice was comparable when food intake was normalized to the body weight (Figure 4E and F). p62 KO aged mice had higher serum ethanol concentrations compared with WT aged mice after Gao-binge alcohol feeding (Figure 4G).

To further evaluate the impact of p62 deficiency on liver injury and steatosis, we measured serum levels of alanine aminotransferase (ALT) and hepatic lipids from all groups. The serum levels of ALT tended to be increased in alcohol-fed WT mice but were comparable between the young and aged mice, suggesting aging alone may not affect alcohol-



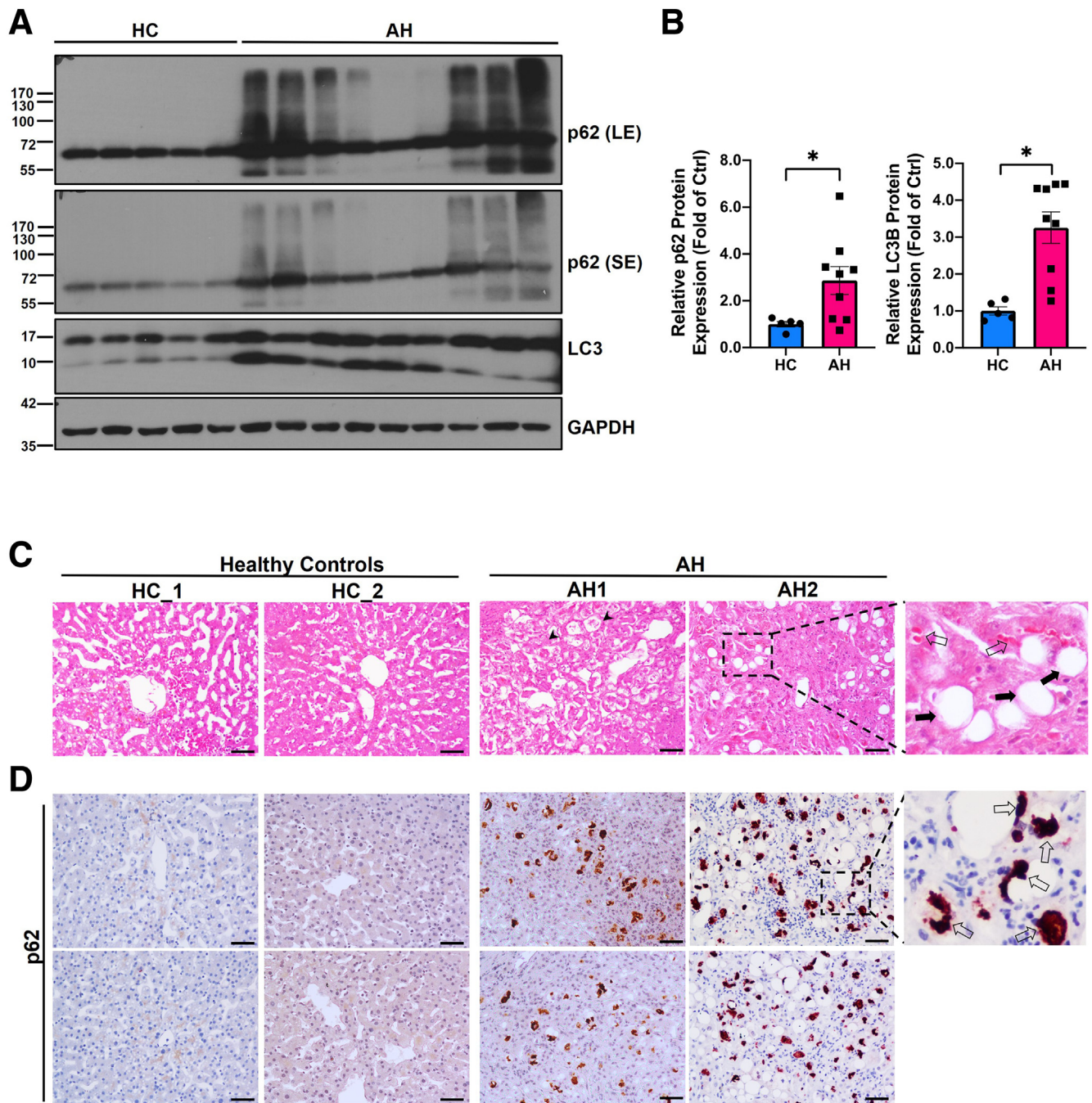
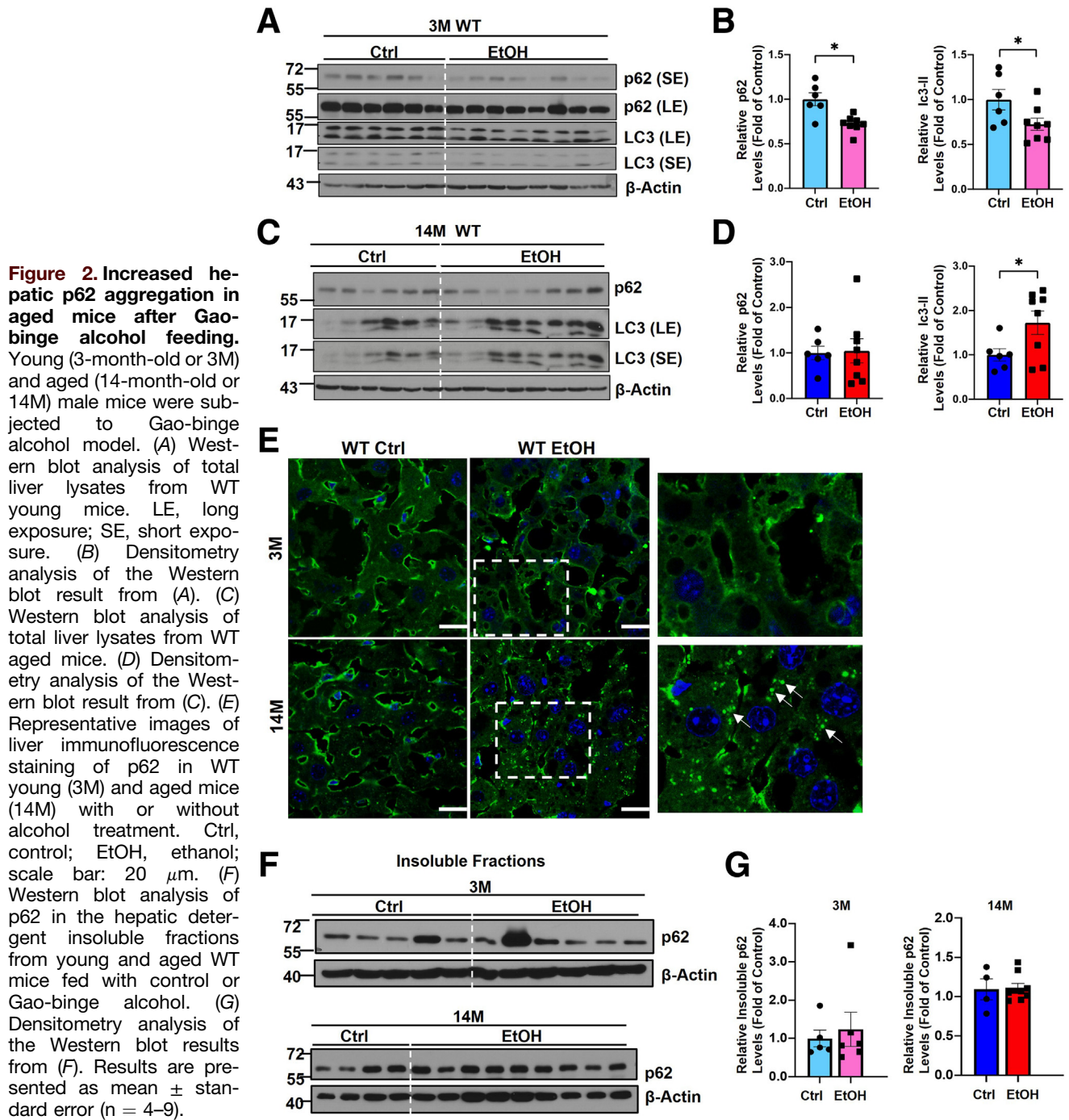


**Figure 1. Increased level of hepatic p62 and its aggregation in patients with alcoholic hepatitis (AH).** (A) Western blot analysis of total liver lysates of healthy donors (normal liver) and AH patients, respectively. LE, long exposure; SE, short exposure. (B) Densitometry analysis of p62 and LC3B expression. Results are presented as mean  $\pm$  standard error ( $n = 5-8$ ).  $*P < .05$  with Student  $t$  test. (C and D) Representative images of H&E and immunohistochemical staining of p62 in liver tissues from AH patients and healthy donors. *Arrowheads*: hepatocyte ballooning; *solid black arrows*: lipid droplets; scale bar: 50  $\mu\text{m}$ .

induced liver injury (Figure 5A). There were no differences in serum levels of ALT among control diet-fed WT and p62 KO mice regardless of age, suggesting aged p62 KO mice did not show increased liver injury despite increased obesity. However, the serum levels of ALT in aged p62 KO mice were significantly higher than the age-matched WT mice after alcohol feeding (Figure 5A), suggesting loss of p62 exacerbates alcohol-induced liver injury. The levels of hepatic TG

were significantly elevated in alcohol-fed mice compared with control diet-fed mice regardless of genotype and age (Figure 5B). Levels of hepatic TG were already significantly higher in control diet-fed aged p62 KO mice than aged WT mice, suggesting that loss of p62 promotes hepatic steatosis during aging (Figure 5B). Alcohol feeding further increased levels of hepatic TG in aged p62 KO mice compared with control diet-fed aged p62 KO mice (Figure 5B). Levels of





hepatic cholesterol remained unchanged among young mice regardless of genotype and alcohol feeding but were significantly increased in aged p62 KO mice and were further elevated by alcohol feeding (Figure 5C). Consistently, results from H&E and Oil Red O staining of the corresponding liver tissues showed that alcohol feeding generally promoted the accumulation of hepatic LD in mice regardless of age and genotypes. Increased hepatic LDs were already evident in control diet-fed aged p62 KO mice, which was further increased by alcohol feeding (Figure 5D and E). Taken together, these data indicate that loss of p62

promotes mature-onset obesity and exacerbates alcohol-induced hepatic steatosis and liver injury in aged mice.

### *Aged p62 Knockout Mice Are Resistant to Alcohol-Induced White Adipose Atrophy but Have Increased Adipose Inflammation*

Alcohol feeding decreased the weight of epididymal white adipose tissue (eWAT) (Figure 6A–C) and reduced the size of adipocytes as assessed by H&E staining in young WT mice (Figure 6D and E). Alcohol-induced eWAT atrophy was

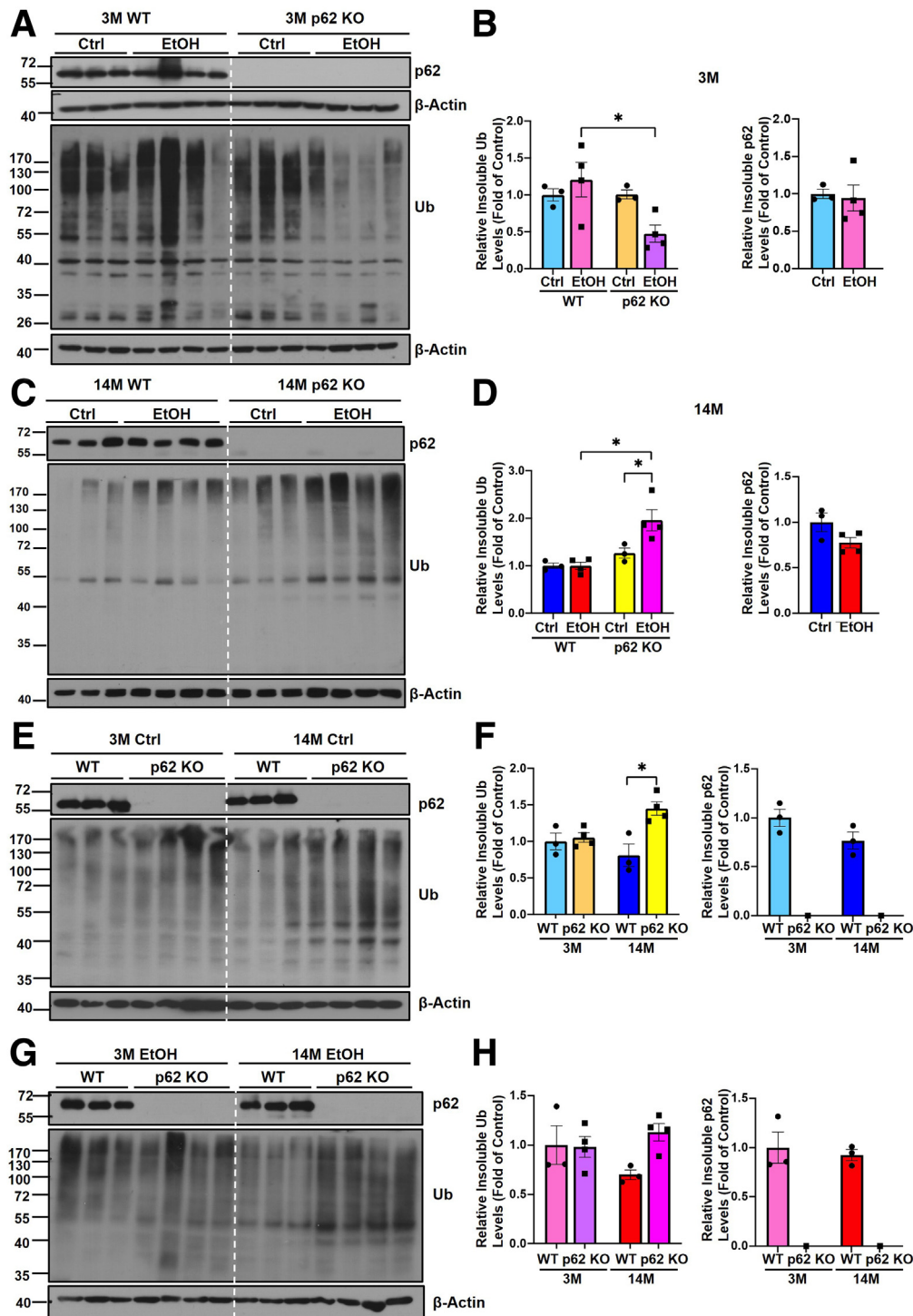


**Figure 3.** The levels of detergent insoluble ubiquitinated proteins in young and aged WT and p62 KO mice with or without Gao-binge alcohol feeding. (A and B) Young (3M) and (C and D) aged (14M) male mice were subjected to Gao-binge alcohol model. Hepatic detergent insoluble fractions were prepared and subjected to Western blot analysis of p62 and ubiquitin (Ub). (B and D) Densitometry analysis of the Western blot results from (A and C), respectively. Western blot analysis of p62 and Ub from hepatic detergent insoluble fractions young and aged mice fed with the control diet (E) or alcohol (G). (F and H) Densitometry analysis of the Western blot results from (E and G), respectively. Results are presented as mean  $\pm$  standard error ( $n = 3-4$ ). \* $P < .05$ ; one-way analysis of variance followed by Tukey post hoc test.

even more evident in aged WT mice (Figure 6A-E). Interestingly, alcohol feeding failed to decrease the weight of eWAT, the ratio of eWAT to body weight, and the size of adipocytes in aged p62 KO mice (Figure 6A-E), suggesting aged p62 KO mice were resistant to alcohol-induced white adipose atrophy. Levels of serum FFAs were significantly higher in alcohol-fed mice regardless of genotype and age (Figure 6F). Levels of serum glycerol were comparable in

young mice regardless of alcohol feeding and genotype but were dramatically increased in alcohol-fed aged p62 KO mice (Figure 6G). Activated mitogen-activated protein kinase (ERK) can enhance the expression of peroxisome proliferator-activated receptor (PPAR)  $\gamma$  and CCAAT/enhancer-binding protein (C/EBP) to promote adipogenesis.<sup>57</sup> Alcohol feeding markedly decreased p62 protein levels but increased phosphorylated ERK in both young and

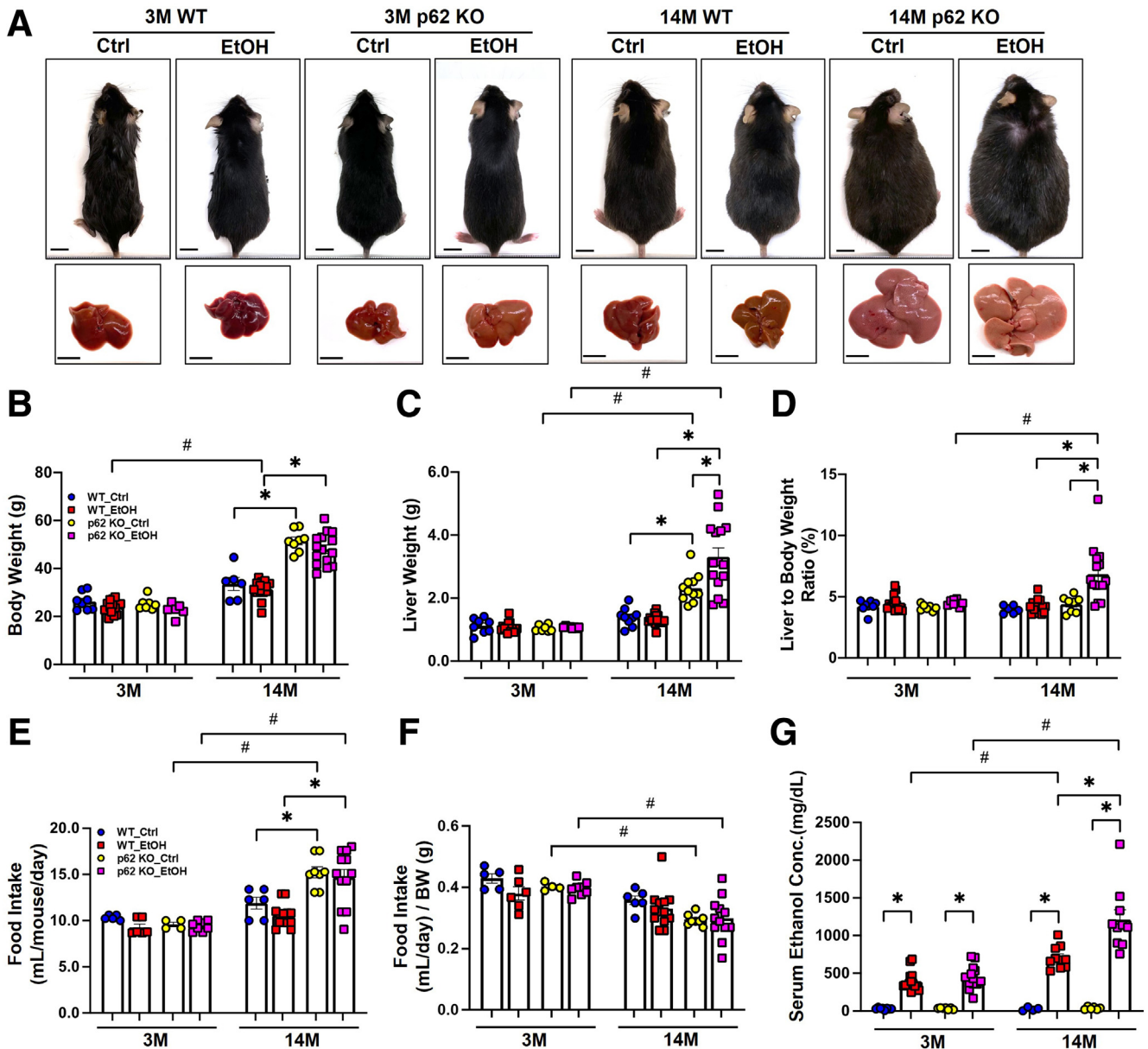


**Figure 4. p62 knockout mice develop mature-onset obesity during aging.** (A) Representative images of the mice and gross anatomy of livers from young and aged mice with the indicated genotype and treatment. Scale bar: 1 cm. (B) Measurement of mice body weight (in grams). (C) Measurement of liver weight (in grams). (D) Liver to body weight (BW) ratio. (E) Average of food intake (in mL) per day per mouse. (F) Normalized food intake by body weight of the mice in each group. (G) Serum ethanol concentration of young and aged mice with the indicated genotype and treatment. Results are presented as mean  $\pm$  standard error ( $n \geq 4$ ). \* $P < .05$ ; # $P < .05$  between young and aged group; one-way analysis of variance followed by Tukey post hoc test.

aged WT mouse eWAT (Figure 7A–D). However, levels of phosphorylated ERK were largely varied among alcohol-fed young p62 KO mice (Figure 7A). Levels of phosphorylated ERK were already higher in control diet-fed aged p62 KO mice, which were not further changed after alcohol feeding compared with age-matched WT mice (Figure 7B). Levels of total ERK decreased in alcohol-fed p62 KO aged mice compared with control diet-fed mice (Figure 7B and D). Hormone-sensitive lipase (HSL) is a key enzyme for adipose tissue lipolysis to mobilize fatty acids from stored TG in adipocytes, which is activated by its phosphorylation.<sup>58</sup> Levels of phosphorylated HSL in eWAT were markedly

increased in both alcohol-fed young WT and p62 KO mice compared with their respective control diet-fed mice (Figure 7A). Intriguingly, although alcohol feeding markedly increased phosphorylated HSL in aged WT mice, HSL phosphorylation was completely blunted in aged p62 KO mice (Figure 7B), suggesting that lacking p62 may inhibit adipose lipolysis in aged mice.

Adipose tissue inflammation can facilitate adipogenesis, adipose tissue expansion and remodeling as an adaptive response.<sup>59</sup> Crown-like structures (CLS) composed of clustering macrophages surrounding dead or dying adipocytes is a histologic hallmark of the proinflammatory process in



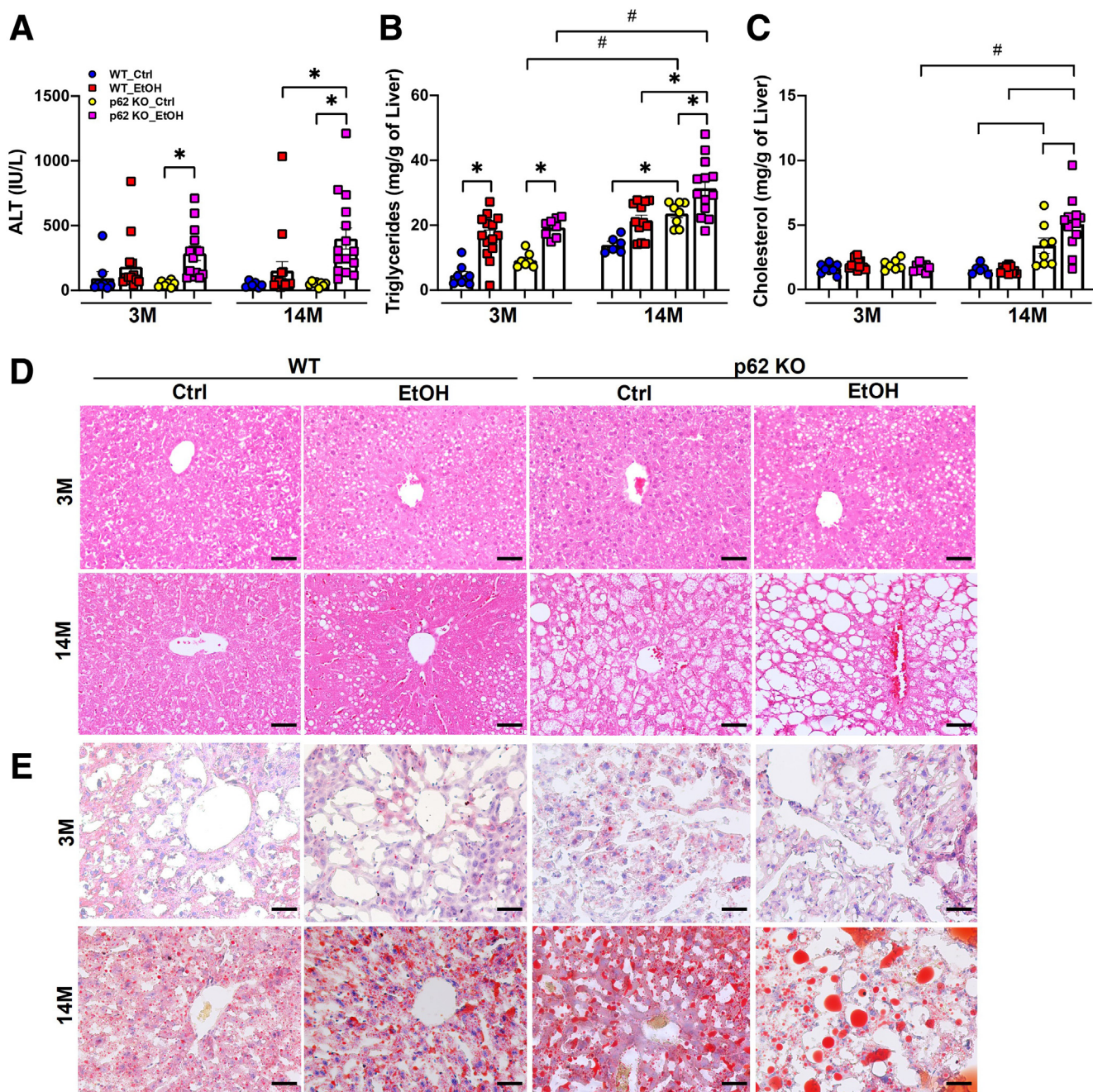


**Figure 5. p62 KO exacerbates alcohol-induced liver injury and steatosis in aged mice.** Levels of serum ALT (A), hepatic triglycerides (B), and hepatic cholesterol (C) in young and aged mice with the indicated genotype and treatment. Results are presented as mean  $\pm$  standard error ( $n \geq 6$ ). \* $P < .05$ , one-way analysis of variance with Tukey post hoc test. (D and E) Representative images of H&E and Oil Red O staining of liver sections from young mice and aged mice with the indicated genotype and treatment. Scale bar: 50  $\mu$ m.

adipose tissue.<sup>60</sup> We found increased number of F4/80 or myeloperoxidase (MPO) positive cells displaying typical CLS in aged p62 KO mice compared with aged WT mice (Figure 8A and B), suggesting that lacking p62 alone may increase adipose tissue inflammation. Although alcohol feeding had little effects on the CLS in aged WT mice, alcohol feeding further increased the number of CLS in p62 KO aged mice (Figure 8A and B). Consistently, the mRNA levels of *Adgre1* (Kupffer cell/macrophage marker) and *Cd68*

(monocytes marker) were significantly increased in aged p62 KO mice irrespective of alcohol feeding (Figure 8C). The mRNA levels of proinflammatory cytokines *Il6* and chemokine *Ccl2* were significantly higher only in the aged p62 KO mice fed with alcohol (Figure 8C), indicating that p62 may play a role in suppressing alcohol-induced adipose inflammation. Together, these results suggest that lacking p62 inhibits alcohol-induced adipose atrophy but promotes alcohol-induced inflammation in aged mouse WAT.

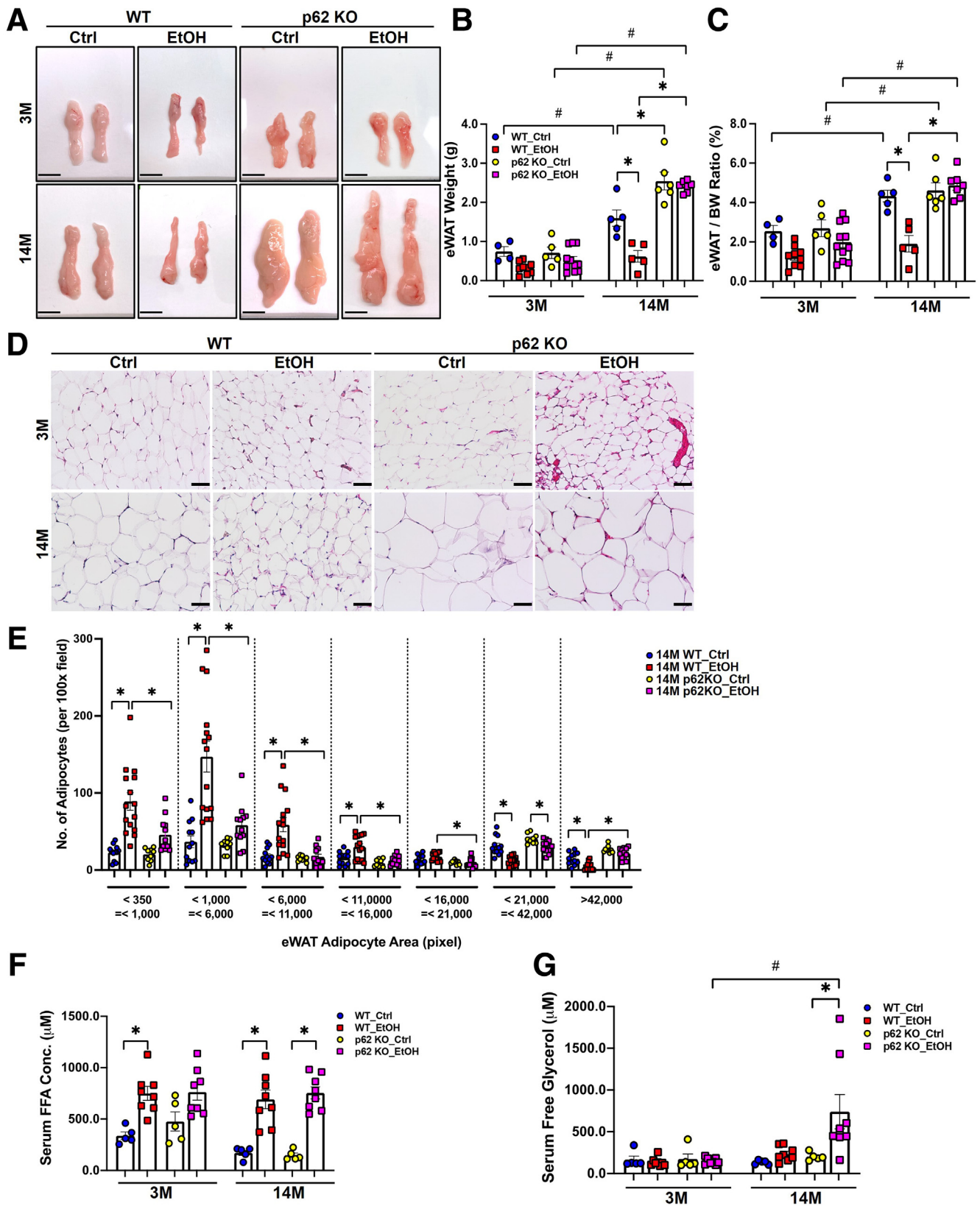


**Figure 6. Gao-binge alcohol induces white adipose tissues atrophy in WT but not p62 KO aged mice.** (A) Representative images of gross anatomy of eWAT (epididymal white adipose tissue) section from mice with the indicated genotype and treatment. Scale bars: 1 cm. (B) Measurement of eWAT (in grams) and (C) eWAT to body weight (BW) ratio. (D) Representative images of H&E of eWAT section from mice with the indicated genotype and treatment. Scale bar: 50  $\mu\text{m}$ . (E) Quantification of the number of eWAT adipocytes with different area (pixel) based on per 100 $\times$  H&E staining. Each dot represents the number of eWAT adipocytes per image, and at least  $n \geq 3$  mice were quantified in each group. (F) Quantification of serum free fatty acids (FFA) concentration and (G) serum free glycerol concentration from mice with the indicated genotype and treatment. Data are presented as mean  $\pm$  standard error ( $n \geq 4$ ). \* $P < .05$ , one-way analysis of variance followed by Tukey post hoc test.



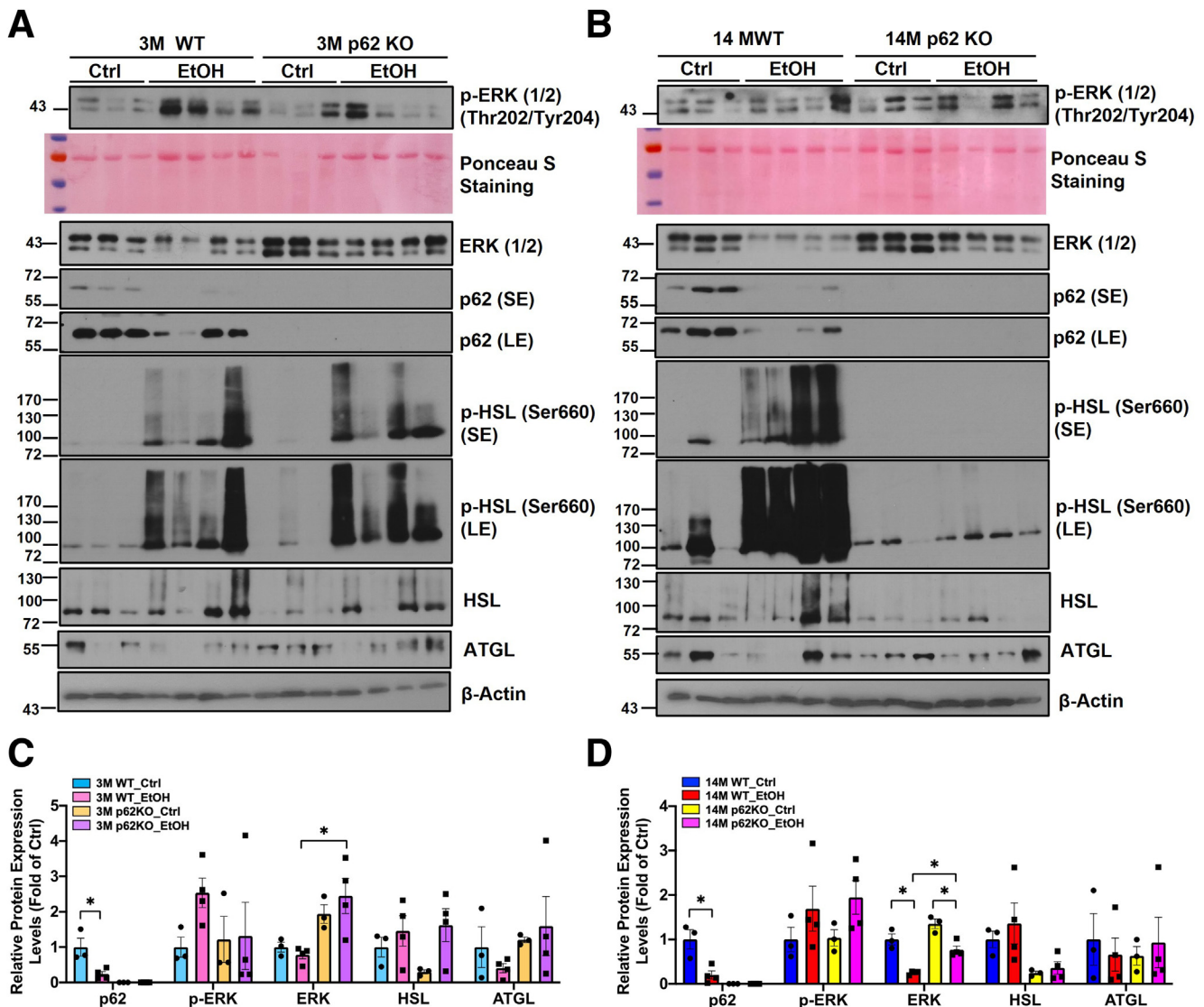


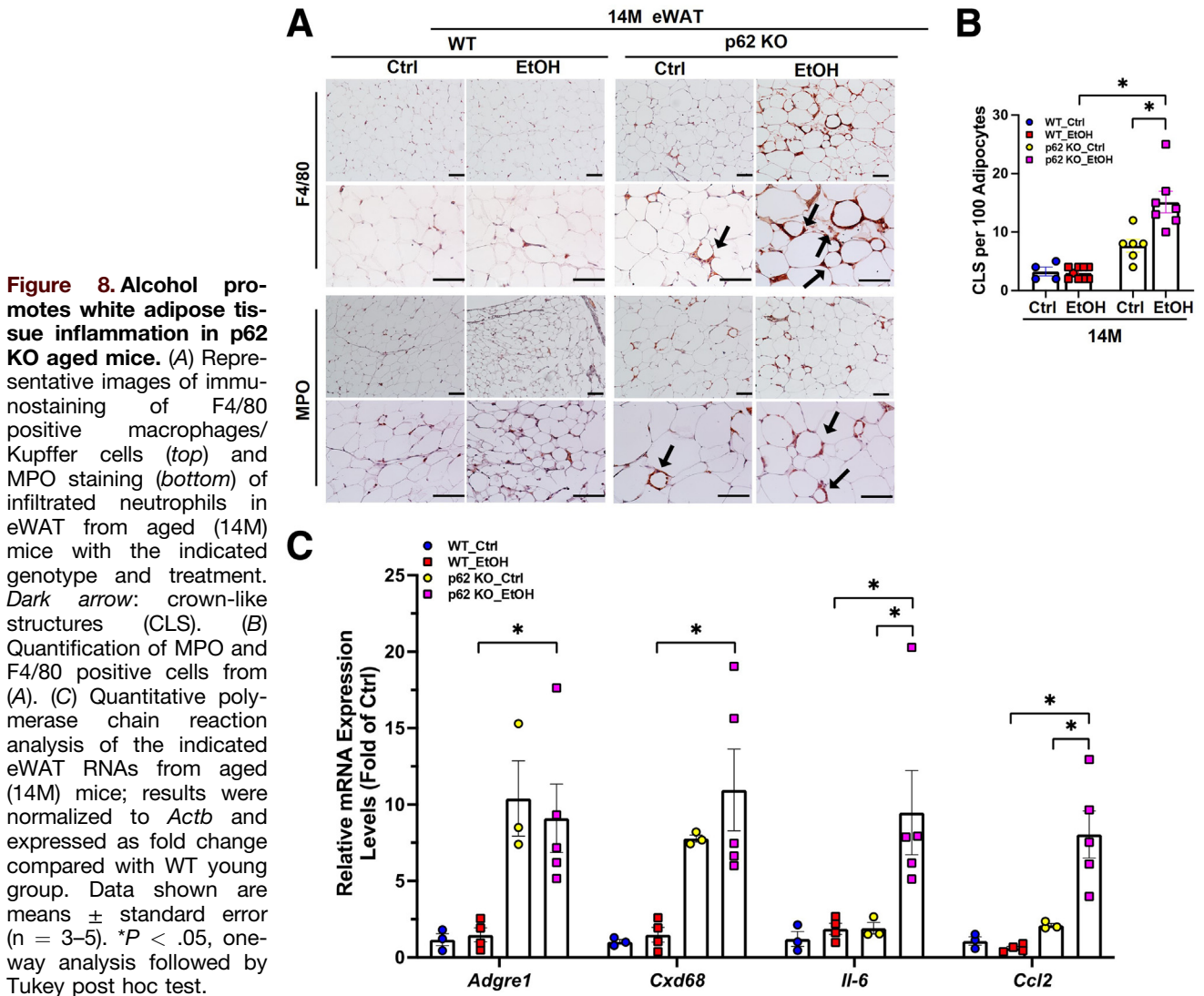
**Figure 7. Alcohol decreases p62 expression and alters adipose lipolysis in eWAT.** (A and B) Western blot analysis of total eWAT lysates from young and aged mice with the indicated genotype and treatment; Ponceau S staining of total proteins is also included. SE, short exposure; LE, long exposure. (C and D) Densitometry analysis of the Western blot results from (A) and (B), respectively. Note that phosphorylated HSL is not included in the quantification because the change is obvious on the blot.

### Aged p62 Knockout Mice Are Maladaptive to Alcohol-Induced Brown Adipose Activation

In contrast to WAT, the main function of BAT is to maintain body temperature homeostasis by oxidizing FFAs and glucose to produce heat.<sup>61</sup> Previous studies showed that alcohol increases thermogenesis, which mitigates alcohol-induced hepatic steatosis and liver injury in mice by increasing the expression of UCP1 in BAT.<sup>48,49</sup> Alcohol feeding decreased BAT weight and the ratio of BAT to body weight in WT and p62 KO young mice, and these changes were more significant in WT aged mice (Figure 9A and B). Alcohol feeding also decreased the weight of BAT but did not significantly affect the ratio of BAT to body weight in aged p62 KO mice compared with the control diet-fed aged p62 KO mice (Figure 9A and B). H&E staining revealed that the number of LDs in BAT decreased dramatically in

alcohol-fed mice regardless of age and genotype, but p62 KO aged mice were less affected compared with the age-matched WT mice (Figure 9C). We next evaluated the thermogenesis by measuring the mRNA levels of thermogenesis-related genes in BAT. PR domain containing 16 (PRDM16) is a transcription factor that regulates the expression of thermogenic genes in BAT.<sup>62</sup> Type 2 iodothyronine deiodinase (DIO2) is a selenoenzyme that increases thyroxine activation to 3,5,3'-triiodothyronine in BAT, resulting in mitochondrial uncoupling and enhanced thermogenesis.<sup>63</sup> Alcohol feeding did not have a significant effect on mRNA levels of *Ucp1* and *Prdm16* but significantly increased the expression of *Dio2* in young WT and p62 KO mice (Figure 9D). Cell death-inducing DNA fragmentation factor (CIDEA) is a LD protein that promotes the enlargement of LDs in BAT.<sup>64</sup> In WT aged mice, alcohol feeding





increased the expression of *Ucp1*, *Prdm16*, *Cidea*, *Cox8b*, and *Ppargc-1a*, but in comparison, the mRNA levels of these genes were significantly lower in p62 aged KO mice (Figure 9D). The mRNA levels of fatty acid oxidation-related genes, carnitine palmitoyltransferase 1a (*Cpt1a*), acyl-coenzyme A oxidase 1 (*Acox1*), acyl-coenzyme A dehydrogenase long-chain (*Acadl*), and acyl-coenzyme A dehydrogenase medium chain (*Acadm*), were dramatically decreased in aged p62 KO mice compared with aged WT mice with alcohol feeding (Figure 9D). These data suggest that p62 is required for alcohol-induced up-regulation of thermogenesis genes in BAT in aged mice.

Similar to eWAT, alcohol feeding slightly decreased levels of p62 and increased LC3-II in BAT. As expected, levels of p62 were completely undetectable in BAT of p62 KO mice (Figure 10A). Alcohol feeding increased the levels of UCP1 up to 2.9-fold in young and 2.5-fold in aged WT mice compared with the respective control diet-fed mice. However, alcohol feeding failed to increase levels of UCP1 in both young and aged p62 KO mice, suggesting p62 may be

required for alcohol-induced UCP1 up-regulation in BAT. Despite there being some variations among the mice, alcohol feeding increased the levels of total activating transcription factor 2 (ATF2) and phosphorylated ATF2 in aged WT mice but not in aged p62 KO mice. Levels of total ATF2 and phosphorylated ATF2 were also lower in alcohol-fed young p62 KO mice than alcohol-fed young WT mice (Figure 10A). Because mitochondria are critical for BAT functions, we next determined the change of mitochondrial proteins in all groups. Levels of PGC1 $\alpha$ , the key transcription co-activator for mitochondria biogenesis, did not change in alcohol-fed WT young and aged mice but were markedly decreased in alcohol-fed young and aged p62 KO mice (Figure 10B). Alcohol feeding increased levels of several mitochondrial proteins including the translocase of the outer membrane protein 20 (TOM20) and several inner membrane proteins of mitochondrial oxidative phosphorylation complexes in young and aged WT mice (Figure 10B and C). The levels of TOM20 decreased, whereas levels of several mitochondrial oxidative phosphorylation complex proteins including

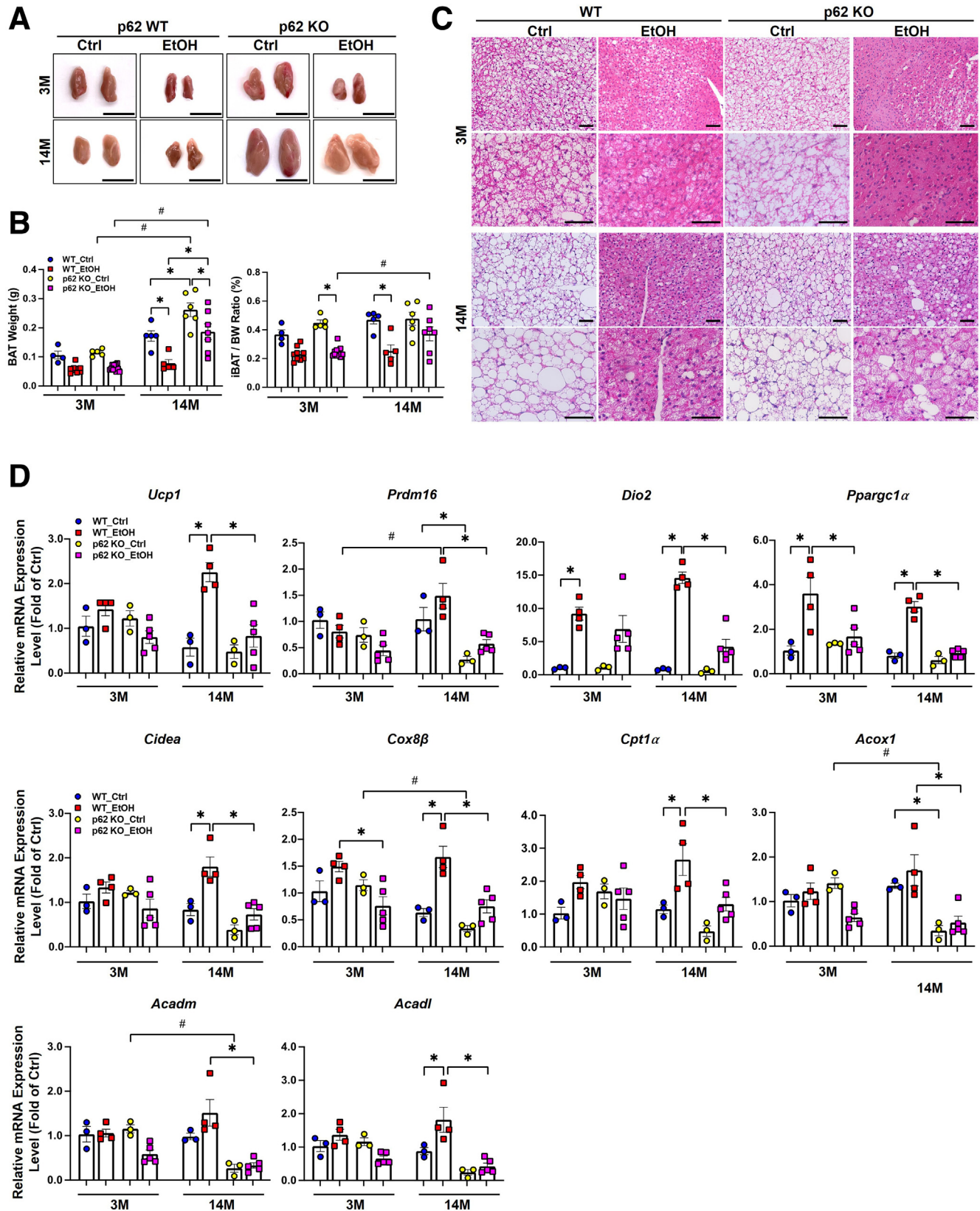


**Figure 9. Impaired BAT activation in aged p62 KO mice fed with Gao-binge alcohol.** (A) Representative images of gross anatomy of BAT (brown adipose tissue) sections from young and aged mice with the indicated genotype and treatment. Scale bars: 1 cm. (B) Measurement of BAT weight (in grams) and BAT to body weight ratio. (C) Representative images of H&E staining of BAT sections from young and mice with the indicated genotype and treatment. Scale bar: 50  $\mu$ m. (D) Quantitative polymerase chain reaction analysis of the indicated mRNAs in BAT sections from young and aged mice with the indicated genotype and treatment. Data are presented as mean  $\pm$  standard error ( $n = 3-5$ ). \* $P < .05$ , \*\* $P < .001$ , # $P < .05$  between young and aged group. One-way analysis of variance followed by Tukey post hoc test.

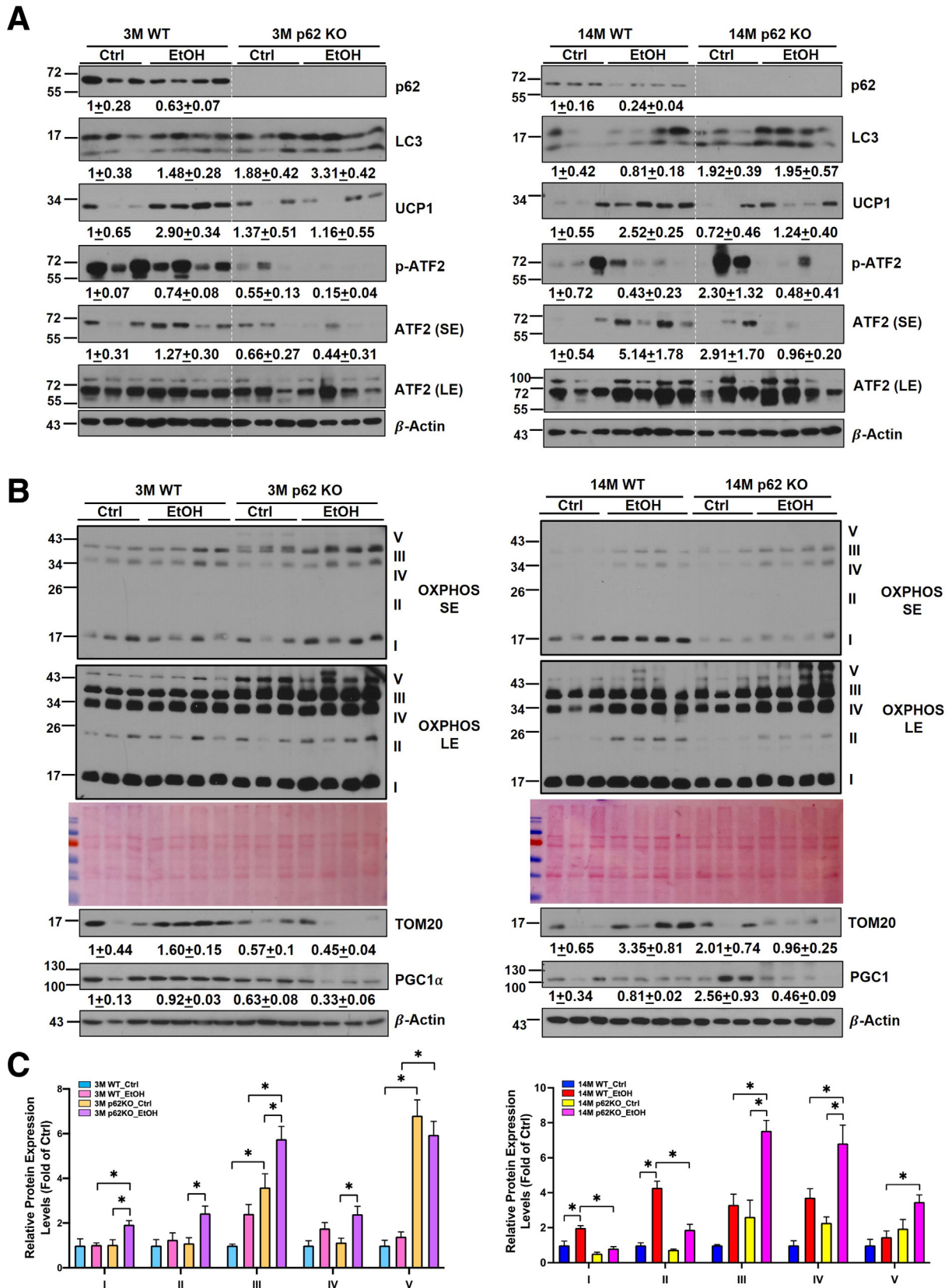


**Figure 10. p62 is required for alcohol-induced BAT activation in mice.** (A and B) Western blot analysis of BAT lysates from young and aged mice with the indicated genotype and treatment. The result of quantification on Western blot is shown below each corresponding band and is presented as fold change, mean ± standard error. (C) Densitometry analysis of OXPHOS from (B). SE, short exposure; LE, long exposure.



complex III, IV, and V were all increased in alcohol-fed young and aged p62 KO mice (Figure 10B), which is likely due to impaired p62-mediated mitophagy. Taken together, these data suggest that Gao-binge alcohol induces BAT activation, which is impaired in p62 KO aged mice.

### Hepatic de Novo Lipogenesis and Fatty Acid Beta Oxidation May Not Be Critical in Gao-Binge Alcohol-Induced Steatosis in Aged Mice

Hepatic protein and mRNA levels of FA synthase (FASN) and acetyl-coA carboxylase  $\alpha$  (ACC $\alpha$ ) decreased in alcohol-fed WT aged mice compared with the aged WT mice fed with control diet (Figure 11A and B), suggesting hepatic de novo lipogenesis may not be critical in Gao-binge alcohol-induced steatosis in aged WT mice. Unlike WT mice, hepatic protein and mRNA levels of *Fasn* and ACC $\alpha$  did not change in alcohol-fed p62 KO aged mice compared with control diet-fed p62 KO mice. Nonetheless, when compared with alcohol-fed WT aged mice, the protein level of FASN and ACC $\alpha$  as well as the mRNA level of *Fasn* were significantly higher in alcohol-fed p62 KO aged mice (Figure 11A–C). Levels of serum  $\beta$ -hydroxybutyrate, one of the products of  $\beta$ -oxidation, were significantly increased by alcohol feeding regardless of age and genotype (Figure 11D), suggesting increased hepatic steatosis in alcohol-fed mice is less likely due to impaired hepatic fatty acid oxidation. Fibroblast growth factor 21 (FGF21) is an endocrine factor that is secreted from liver and other metabolic tissues, which is critical for the induction of fatty acid oxidation, ketogenesis, and gluconeogenesis in response to starvation and alcohol consumption.<sup>65–67</sup> Alcohol feeding significantly increased the mRNA levels of hepatic *Fgf21* in WT but not p62 KO aged mice (Figure 11E). However, serum levels of FGF21 increased significantly in both alcohol-fed aged WT and p62 KO mice, although the levels of FGF21 were slightly lower in alcohol-fed p62 KO aged mice than alcohol-fed WT aged mice (Figure 11F). Together, these data suggest hepatic de novo lipogenesis and fatty acid oxidation may not be critical in alcohol-induced steatosis in aged mice with or without p62.

### p62 KO Aged Mice Exhibit Elevated Secretion of Proinflammatory and Angiogenic Adipokines

Adipose tissue not only stores fat but also secretes circulating hormones and inflammatory cytokines.<sup>68</sup> To determine the effect of p62 and aging on adipose tissue secretome, we used Proteome Profiler mouse adipokine antibody arrays to examine the changes of mouse serum adipokines in young and aged mice. Among 38 adipokines that we tested, we identified 10 serum adipokines that showed obvious change in alcohol-fed aged WT and p62 KO mice (Figure 12A). Levels of serum adiponectin, one of the main adipokines, remained relatively unchanged in alcohol-fed WT aged mice but were slightly decreased in young and p62-KO aged mice after alcohol feeding (Figure 12B). The basal levels of leptin in control diet-fed p62 aged KO mice were significantly higher than the aged WT mice. Serum levels of leptin decreased in aged WT mice but were

increased dramatically in aged p62 KO mice (Figure 12B). Because p62 KO aged mice have severe obesity, these data suggested that the p62 KO aged mice might have developed leptin resistance. Strikingly, serum levels of chemokine (C-C motif) ligand 2 (CCL2), retinol-binding protein-4 (RBP4), tissue inhibitor of metalloproteinases-1 (TIMP-1), FGF acidic, hepatocyte growth factor (HGF), preadipocyte factor-1 (Pref-1), serpin E1 (also known as plasminogen activator inhibitor-1), and vascular endothelial growth factor (VEGF) were all increased in alcohol-fed aged p62 KO mice compared with other groups (Figure 12B and C). The change of these adipokines was moderate in young mice regardless of genotype (Figure 12B and C). These data suggest that p62 may play a role in regulating systemic inflammation during alcohol-induced stress in aged mice.

We next investigated inflammation-related processes in the liver including macrophage accumulation, infiltration of neutrophils, and hepatic expression of inflammatory cytokines. In WT aged mice, alcohol feeding reduced the number of F4/80-positive macrophages. However, the number of F4/80-positive macrophages was already less in p62 KO aged mice than that in control diet-fed WT aged mice, and alcohol feeding did not have a further impact (Figure 13A and B). The number of activated CD68-positive macrophages was significantly increased in both WT and p62 KO aged mice after alcohol feeding, but no difference was found between alcohol-fed WT and p62 KO mice (Figure 13A and B). In WT aged mice, alcohol feeding generally down-regulated the mRNA levels of the inflammation-related genes including *Adgre1*, *Cd68*, *Il6*, *Il1b*, *Ccl2*, and *Sele* (Figure 13C). Interestingly, alcohol feeding did not decrease the expression levels of these genes in p62 KO aged mice. More importantly, the expression levels of *Il6* and *Ccl2* increased (~3-fold) in p62 KO mice compared with WT mice after alcohol feeding (Figure 13C). Together with the inflammation data in adipose tissue (Figure 8), these results suggest that loss of p62 in aged mice aggravates alcohol-induced inflammation response in mouse adipose and liver tissues.

## Discussion

Aging is associated with various types of chronic liver diseases including ALD.<sup>69</sup> p62 has been implicated in various aging-related diseases, where it mainly plays a protective role against a wide variety of aging-related processes.<sup>70–72</sup> The expression of p62 is dramatically decreased in the brain of patients with Alzheimer's disease, one common age-associated neurodegenerative disease.<sup>73</sup> Co-expression of p62 and senescent markers p16 or p21 was observed in inflamed small bile ducts in primary biliary cirrhosis.<sup>74</sup> Aging decreases hepatic SIRT1 signaling and impairs alcohol metabolism, autophagy, and lysosomal degradation as well as liver regeneration; all of these can exacerbate ALD.<sup>17–20,34</sup> In addition, alcohol consumption also disturbs the normal functions of adipose tissue, which leads to increased adipose lipolysis and secretion of adipokines and cytokines, which contributes to ALD.<sup>45,46,75,76</sup> Obesity and alcohol consumption synergistically increase



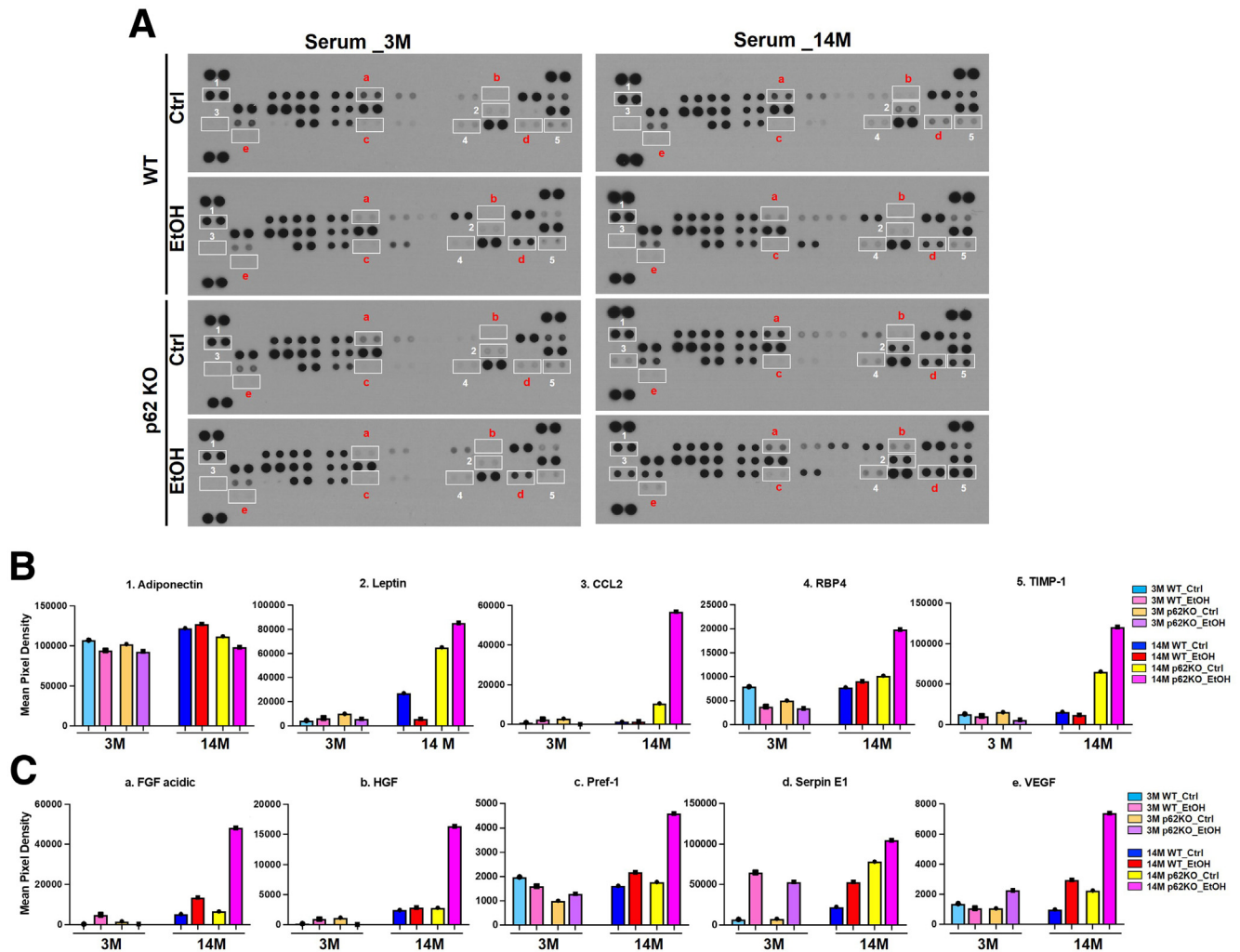
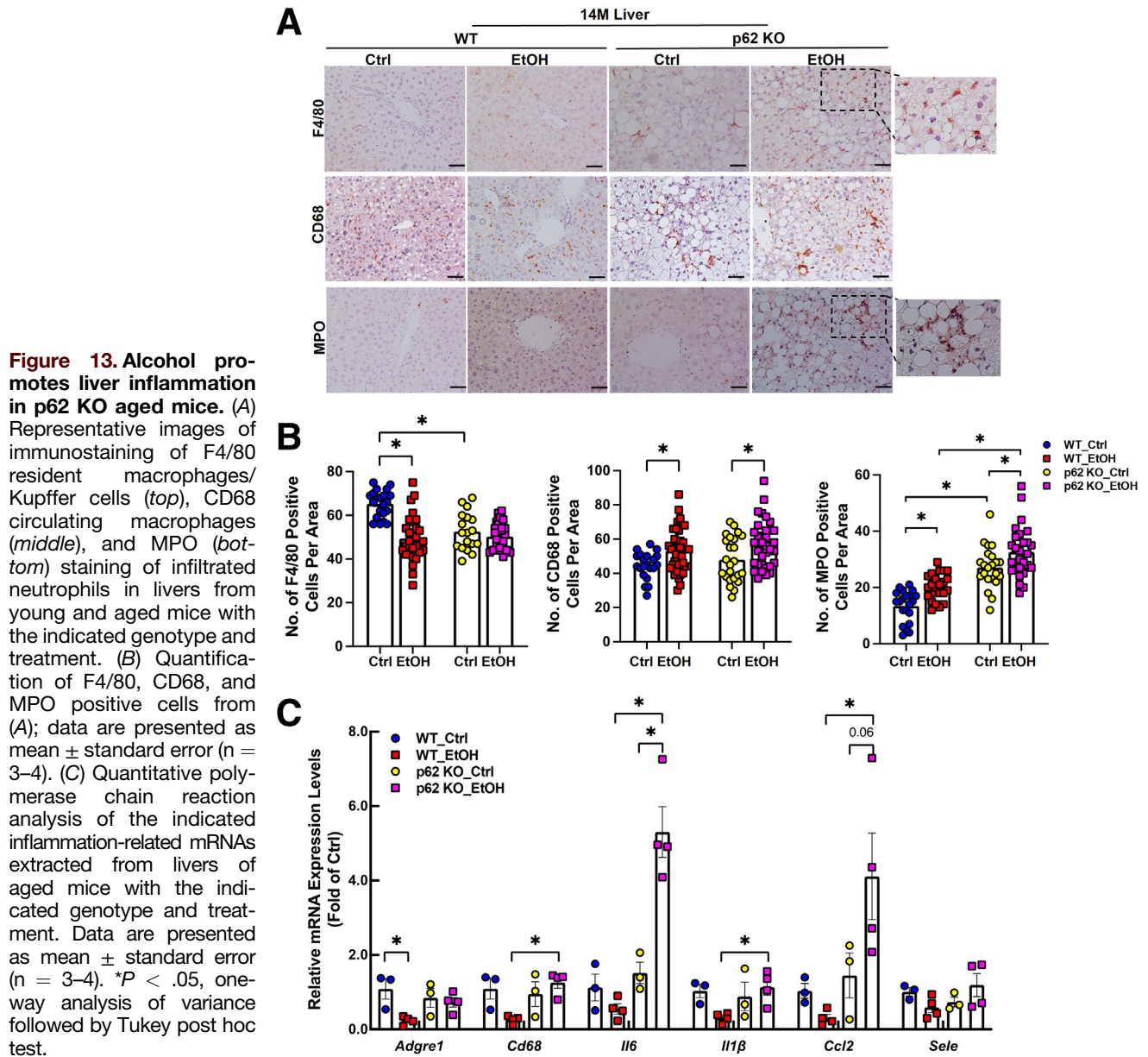


**Figure 12.** Effects of alcohol on adipokine secretion in mice. Young (3M) and aged (14M) male p62 KO mice and their age-matched WT littermates were subjected to Gao-binge alcohol model. (A) Representative results of adipokine array assay on the serum from young and aged mice with the indicated genotype and treatment. Serum from different groups were assessed for adipokine expression using an antibody adipokine array, where each group consists of the serum collected from 8 mice. (B and C) Densitometry analysis of the adipokine array result from (A).

induced lipolysis.<sup>79</sup> Our findings that ethanol-feeding increases levels of serum FGF21 and levels of phosphorylated HSL in WAT are generally in agreement with the previous reports.<sup>47,79</sup> Intriguingly, our findings suggest that loss of p62 in young mice does not have a significant impact on WAT lipolysis. However, aged p62 KO mice have significantly higher levels of serum glycerol but not FFA compared with aged WT mice after ethanol feeding. There are several possibilities to explain this observation. Although aged p62 KO mice have bigger WAT mass, the levels of serum glycerol (presumably from adipose lipolysis) are comparable between control diet-fed aged WT and p62 KO mice, suggesting that p62 may not have a significant impact on the basal level of lipolysis. The reasons on increased serum levels of glycerol in ethanol-fed aged p62 KO mice remain unclear but could be due to the out of balance of increased adipogenesis and lipolysis in the p62 aged KO mice. The WAT mass was bigger in aged p62 KO mice, which may also

be partially responsible for the increased serum levels of glycerol. Aged p62 KO mice have markedly decreased levels of phosphorylated HSL and relatively low FGF21 compared with aged WT mice after ethanol feeding, suggesting aged p62 KO mice have decreased response to  $\beta$ -adrenergic receptor-stimulated lipolysis likely as a negative feedback response to counteract the increased mass of adipose tissue. Whole-body p62 KO mice have increased food intake and glucose and insulin intolerance as well as leptin resistance.<sup>50</sup> We found that p62 KO mice consumed more control and alcohol diet with increased serum levels of leptin. Moreover, the levels of phosphorylated ERK increased in aged p62 KO mice regardless of alcohol feeding, which is also consistent with the previous report that increased ERK activation promotes adipogenesis in p62 KO mice.<sup>50</sup> Using a comprehensive Cre approach to delete p62 specifically in multiple tissues, it is shown that deletion of p62 in adipose but not liver, muscle, central nervous system, or myeloid





tissue can recapitulate the obese phenotypes of the whole-body p62 KO mice.<sup>51</sup> ATF2 binds to the promoter of *Ppargc1α* and *Ucp1*. During  $\beta$ -adrenergic stimulation, ATF2 is phosphorylated by p38 and translocated to the nucleus to increase the expression of *Ppargc1α* and *Ucp1*.<sup>80</sup> Deletion of p62 in BAT induces abnormal mitochondria structures and mitochondrial dysfunction, with decreased levels of PGC1 $\alpha$  and UCP1 due to impaired p38-ATF2 activation resulting in impaired thermogenesis and energy expenditure.<sup>51,52</sup>

It has been reported that alcohol consumption activates BAT by increasing the expression of *Ucp1* likely by hypothalamic neural circuits and sympathetic innervating BAT as an adaptive response to protect against ALD.<sup>48</sup> Alcohol-induced BAT activation is also partially mediated by bile acid-mediated TGR5 activation. Whole-body *Tgr5* KO and BAT-specific *Tgr5* knockdown mice blunted alcohol-induced

BAT activation and energy expenditure, which were more susceptible to alcohol-induced liver injury.<sup>49</sup> In addition to increased energy expenditure, BAT may also protect against alcohol-induced liver injury by secreting hepatoprotective adipokines because BAT-specific *Ucp1* KO mice had decreased serum levels of medium molecular weight adiponectin and increased liver injury compared with alcohol-fed WT mice.<sup>48</sup> We found that aged p62 KO mice had decreased serum levels of adiponectin but increased levels of serum proinflammatory cytokines/chemokines, blood clotting factors, and growth hormones, which may contribute to the exacerbated liver injury in alcohol-fed aged p62 KO mice. It is likely that some of the phenotypes are associated with the decreased p38-ATF2 mediated BAT remodeling and mitochondrial changes in p62 KO aged mice. Notably, although the role of p62 in selective

mitophagy is still controversial, it is also likely that loss of p62 may impair mitophagy in BAT because we observed several mitochondrial oxidative phosphorylation complex proteins accumulated in p62 KO mice. It also remains unclear why alcohol-induced BAT changes were only markedly affected in aged but not young p62 KO mice. The exact mechanisms need to be further investigated in the future. Despite many of these unknowns, it seems clear that decreased BAT activation in alcohol-fed p62 aged KO mice may aggravate alcohol-induced liver injury.

Previous studies showed that adipose-specific *Atg7* KO mice have decreased WAT mass but increased BAT mass and are resistant to diet-induced obesity.<sup>81,82</sup> Because adipose autophagy defective mice have increased levels of p62, PGC1 $\alpha$ , and UCP1 in the adipose tissue and adipose-specific p62 KO have decreased levels of PGC1 $\alpha$  and UCP1 with increased obesity,<sup>51,81,82</sup> these vigorously correlated observations indicate that p62 may have anti-obesity functions. Indeed, adipose-*Atg5* KO mice have decreased WAT mass and increased mitochondrial contents, which are resistant to alcohol-induced liver injury.<sup>47</sup>

What is the role of hepatic p62 in the pathogenesis of ALD during aging? It has been generally thought that soluble oligomeric proteins are toxic to the cells. p62 may promote the formation of insoluble protein aggregates because of the ability of p62 to bind with ubiquitinated proteins as an adaptive response to reduce cellular proteotoxicity. It should also be noted that p62 is also reported to be involved in phase separation or forming gel-like p62 bodies or p62 condensates.<sup>55,56</sup> Although immunofluorescence staining for p62 showed increased hepatic p62 positive aggregates in alcohol-fed aged mice, we found no difference in the levels of p62 in the detergent insoluble fractions in either young or aged mice regardless of alcohol feeding. One possible explanation for these differences is that the detergent we used (2% sodium dodecyl sulfate) may not efficiently solubilize the p62 aggregates that we observed in the immunofluorescence staining. It is likely what we observed in the p62 insoluble fractions from the Western blot analysis may reflect the gel-like p62 bodies or p62 condensates but not protein aggregates or MDBs. Because alcohol alone is not sufficient to induce MDBs in mouse livers, future studies are needed to further dissect the role of p62 and the nature of these protein aggregates in the liver by combining alcohol with other diets that are known to induce MDBs. Finally, because aged p62 KO mice are obese and have increased hepatic steatosis, future studies are also needed to determine whether increased hepatic lipids and lipotoxicity would also impact on the ubiquitinated protein aggregates or condensates.

In conclusion, loss of p62 in aged mice leads to obesity with metabolic syndrome-like alterations that exacerbate alcohol-induced liver injury via impaired BAT adaption. Activation of p62-mediated BAT adaption may improve the pathogenesis of ALD.

## Materials and Methods

### Animal Experiments

Whole-body p62 KO mice were generated by Dr Thomas Rüllicke' lab and characterized in Kurt Zatloukal's lab as

described previously.<sup>39,83</sup> p62 KO mice were back crossed to C57BL/6J background for more than 9 generations before they were used for the experiment. All mice were specific pathogen free and received human care in a barrier rodent facility under standard experimental conditions (room temperature 22°C  $\pm$  1°C, relative humidity 50%  $\pm$  10%, and 12-hour dark and light cycles). All procedures were approved by the Institutional Animal Care and Use Committee of the University of Kansas Medical Center. p62 KO and their matched WT young (approximately 3 months) and aged (approximately 14 months) littermates were subjected to chronic plus binge (Gao-binge) alcohol model as described previously.<sup>84,85</sup>

Briefly, mice were acclimated to the Lieber-DeCarli liquid control diet (F1259SP, Bio-Serv) for 5 days, followed by further feeding with the liquid control or ethanol diet (F1258SP, Bio-Serv, 5% ethanol) for 10 days. The volume of control diet given to mice was matched to the volume of ethanol diet consumed. On the last day of feeding, mice were further given 5 g/kg ethanol or 9 g/kg maltose dextran and killed 8 hours later. Blood, liver tissues, and adipose tissues were collected for biochemical and histologic analysis.

### Human Samples

The human normal and AH liver tissues were obtained from the Clinical Resource for Alcoholic Hepatitis Investigations at John Hopkins University. The detailed information of research and samples was listed as previously described.<sup>37</sup>

### Serum Lipid and Other Biochemical Analysis

Serum levels of ALT (Pointe Scientific, cat #A7526), glycerol (Biovision, cat #K630-100), FFA (BioVision, cat #K612-100), and serum ethanol concentrations (Pointe Scientific, cat #A7504) were determined according to the manufacturer's protocols. Serum FGF21 levels were measured by using a commercial enzyme-linked immunosorbent assay kit (R&D Systems, cat #MF2100). Hepatic TG (Pointe Scientific, cat #T7532) and cholesterol (Pointe Scientific, cat #C7510) were determined as previously described.<sup>85,86</sup>

### Adipokine Profiling

The Proteome Profiler Mouse Adipokine Array Kit (ARY013, R&D Systems, Wiesbaden, Germany) detecting 38 adipokines was used to determine the serum adipokine profile. Mouse serum from 8 mice were pooled (10  $\mu$ L from each mouse) and processed according to the manufacturer's instructions. Densitometry analysis of blots was quantified by using DotBlot\_Analysis.ijm Macro from Image J software (National Institutes of Health, Bethesda, MD). Results were corrected for background signals (negative control spots).

### Histology and Immunohistochemistry

Paraffin-embedded liver or adipose tissue sections were deparaffinized, rehydrated, and then incubated with 3%

hydrogen peroxide (Fisher Chemical, cat #H323500), blocking endogenous peroxidase activity, for 10 minutes at room temperature. The tissue sections were stained with different primary and second antibodies (antibodies are listed in Table 1) and then visualized with NovaRed HRP substrate (Vector Labs, cat #SK4805). After visualization with NovaRed, the tissue sections were counterstained with hematoxylin (RICCA, cat #3530-32). Finally, the slides were covered with the mounting medium (Thermo Scientific, 8310-16) and observed under a Nikon microscope. Five-micrometer sections were used for different staining, and the numbers of MPO, CD68, or F4/80 positive cells were counted from 5–8 different fields (200×) per mouse in a double-blinded fashion. The detailed antibody information is listed in Table 1.

### Lipid Droplets Staining

For Oil Red O staining, 5- $\mu$ m frozen section of liver tissue was washed twice with phosphate-buffered saline and then incubated with 60% isopropanol for 1 minute. Tissues were dried in a 37°C incubator for approximately 10 minutes before incubating with Oil Red O solution. Oil Red O solution was prepared by adding 0.35 g Oil Red O (Sigma-Aldrich, cat

#0625) to 100 mL 100% isopropanol, which was further diluted 1.7 times in water and filtered immediately before use. Slides were incubated with Oil Red O solution for 15 minutes. The Oil Red O solution was aspirated from the slides, and 60% isopropanol was added to the slides for several minutes to remove any residual Oil Red O. Slides were washed in phosphate-buffered saline and stained for 30 seconds with hematoxylin, followed by more washes in ddH<sub>2</sub>O. Slides were mounted with a mounting medium (glycerol in phosphate-buffered saline 6:1), followed by microscopy.

### Detergent Soluble and Insoluble Protein Extraction and Western Blot Analysis

The detailed procedure for soluble and insoluble protein extraction has been described previously.<sup>87</sup> Briefly, livers were homogenized in Triton X-100 lysate buffer (0.25 mol/L sucrose, 10 mmol/L Hepes, pH 7.5, 1% Triton X-100, 150 mmol/L NaCl, and freshly add 1 mmol/L DTT when used) and then vortexed and lysed samples on ice for 15 minutes, followed by sonication (3 × 15 seconds). Lysates were then centrifuged for 10 minutes at 14,000 rpm in a micro-centrifuge at 4°C. The supernatants were collected as Triton

**Table 1.** List of Commercial Antibodies Used in This Study

Antibodies	Supplier	Catalogue number
$\beta$ -Actin	Sigma-Aldrich	A5441
ACC $\alpha$	Cell Signaling	3676
p-ACC $\alpha$ (Ser79)	Cell Signaling	3661
ATF2	Cell Signaling	35031S
p-ATF2 (Thr71)/ATF-7 (Thr53)	Cell Signaling	27934S
ERK	Cell Signaling	9102
p-ERK (Thr202/Tyr204)	Cell Signaling	9101
F4/80	Invitrogen	14-4801
FASN	Cell Signaling	3180S
GAPDH	Cell Signaling	2118
p-HSL (ser660)	Cell Signaling	4126S
LC3	PMID: 27151180	
MPO	BioCare Medical	PP023AA
p38	Cell Signaling	9212S
p-p38 (Thr180/Tyr182)	Cell Signaling	4631S
p62	Abnova	H00008878-M01
PPARGC1A	Abnova	PAB12061
OXPPOS cocktail	Abcam	ab110413
Tom20 (FL-145)	Santa Cruz	sc-11415
Ubiquitin (P4D1)	Santa Cruz	Sc-8017
UCP1	Abcam	ab10983
Alexa Fluor 488-goat anti-mouse	Jackson Immuno Research	115-545-146
HRP-goat anti-rabbit	Jackson Immuno Research	111-035-144
HRP-goat anti-mouse	Jackson Immuno Research	115-035-146
HRP-horse anti-mouse	Vector Laboratories	MP-7422
HRP-goat anti-rat	Vector Laboratories	MP-7444
HRP-horse anti-rabbit	Vector Laboratories	MP-7401



**Table 2.** List of Primers Used for Real-Time Polymerase Chain Reaction

Gene	Forward primer (5'–3')	Reverse primer (5'–3')
<i>Accα</i>	CTCCAGGACAGCACAGATCA	TGACTGCCGAAACATCTCTG
<i>Acox1</i>	CAGGAAGAGCAAGGAAGTGG	CCTTTCTGGCTGATCCCATA
<i>Adgre</i>	CTTTGGCTATGGGCTTCCAGTC	GCAAGGAGGACAGAGTTTATCGTG
<i>Atgl/pnpla2</i>	GAGCCCCGGGTGGAACAAGAT	AAAAGGTGGTGGCAGGAGTAAGG
<i>Ccl2</i>	CAGGTCCTGTCTGCTTCT	TCTGGACCCATTCTTCTTG
<i>Cxd68</i>	TGCGGCTCCCTGTGTGT	TCTTCCTGTTCCTTGGGCTAT
<i>Cidea</i>	CTCGGCTGTCTCAATGTCAA	GGGATGGCTGCTTCTCTGTA
<i>Cox8β</i>	GAACCATGAAGCCAACGACT	GCGAAGTTCACAGTGGTTCC
<i>Cpt1α</i>	CCAGGCTACAGTGGGACATT	GAACTTGCCCATGTCTTGT
<i>Dio2</i>	CAGTGTGGTGCACGTCTCAA TC	TGAACCAAAGTTGACCACCAG
<i>Fasn</i>	TGGGTCTAGCCAGCAGAGT	ACCACCAGAGACCGTTATGC
<i>Hsl/lipase</i>	GCCGGTGACGCTGAAAGTGGT	CGCGCAGATGGGAGCAAGAGGT
<i>Lcad</i>	CATTGGTGGGACTTGCTCT	TGGCTATGGCACCGATACAC
<i>Il1b</i>	GCCCATCCTCTGTGACTCAT	AGGCCACAGGTATTTTGTCTG
<i>Il6</i>	ACAACCACGGCCTTCCCTACTT	CATTTCCACGATTTCCAGAGA
<i>Mcad</i>	AGGTTTCAAGATCGCAATGG	CTCCTTGGTGTCTCCACTAGC
<i>p62</i>	AGAATGTGGGGGAGAGTGTG	TCGTCTCCTCCTGAGCAGTT
<i>Pgc1α</i>	ATGTGTGCGCTTCTTGCTCT	ATCTACTGCCTGGGGACCTT
<i>Pparα</i>	ATGCCAGTACTGCCGTTTTT	GGCCTTGACCTTGTTCATGT
<i>Pparγ</i>	TTTTCAAGGGTGCCAGTTTC	AATCCTTGGCCCTCTGAGAT
<i>Prdm16</i>	CAGCACGGTGAAGCCATTC	GCGTGCATCCGCTTGTG
<i>Ucp1</i>	AGGCTTCCAGTACCATTAGGT	CTGAGTGAGGCAAAGCTGATTT
<i>β-actin</i>	TGTTACCAACTGGGACGACA	GGGGTGTGAAGGTCTCAA
<i>36B4</i>	TAAAGACTGGAGACAAGGTG	GTGTACTCAGTCTCCACAGA

X-100 soluble fraction without disrupting the pellet. Pellets were reconstituted in 2% sodium dodecyl sulfate, followed by sonication (3 × 15 seconds), and the lysates were further spun for an additional 5 minutes at 14,000 rpm in a microcentrifuge at room temperature. The supernatants were collected as Triton X-100 insoluble fraction (Insoluble). The protein concentrations were quantified using BCA (Pierce Protein Reagent Assay BCA Kit, 23228). Total liver lysate (30 μg/well) or total adipose tissue lysate (15 μg/well) from each sample was separated by sodium dodecyl sulfate-polyacrylamide gel electrophoresis, transferred to polyvinylidene difluoride membranes, and blocked with 5% non-fat milk in tris-buffered saline tween at room temperature for 1 hour with shaking. Membranes were probed with various primary and secondary antibodies, and the protein bands were developed with SuperSignal West Pico plus chemiluminescent substrate (Thermo Scientific, cat #34578). The detailed antibody information is listed in Table 1. The Western blot results were analyzed by ImageJ.

### RNA Extraction and Real-Time Polymerase Chain Reaction

RNA was isolated from liver tissue or adipose tissue with TRIzol Reagent (Invitrogen, cat #15596018) according to the manufacturer's instructions. RNA concentration and quality were determined by spectrophotometer, and the complementary DNA was prepared as described.<sup>88</sup> Real-time polymerase chain reaction was used to determine

mRNA levels of target genes using a Bio-Rad CFX384 Touch Real-Time PCR Detection System with 2x SYBR Green qPCR Master Mix (Bimake, B21202). *Actb* was used for normalization of liver tissues. The sequences of primers are listed in Table 2.

### Statistical Analysis

All data obtained were analyzed using GraphPad Prism software version 9.0 (GRAPH PAD Software Inc, California). Data were analyzed by Student *t* test for 2-group comparison, One-way analysis of variance with Tukey honestly significant difference post hoc test for multigroup comparison was used to evaluate the statistical differences by GraphPad. The value of *P* critical value  $\leq P$  ( $\alpha = 0.05$ ) was considered statistically significant difference among groups. All experiments data were reported as mean  $\pm$  standard error.

### References

- Paik JM, Golabi P, Younossi Y, et al. Changes in the global burden of chronic liver diseases from 2012 to 2017: the growing impact of NAFLD. *Hepatology* 2020; 72:1605–1616.
- Mokdad AH, Marks JS, Stroup DF, et al. Actual causes of death in the United States, 2000. *JAMA* 2004; 291:1238–1245.
- Peery AF, Crockett SD, Murphy CC, et al. Burden and cost of gastrointestinal, liver, and pancreatic diseases in

- the United States: update 2021. *Gastroenterology* 2022; 162:621–644.
- Bruha R, Dvorak K, Petrtyl J. Alcoholic liver disease. *World Journal of Hepatology* 2012;4:81.
  - Nagy LE, Ding WX, Cresci G, et al. Linking pathogenic mechanisms of alcoholic liver disease with clinical phenotypes. *Gastroenterology* 2016;150:756–768.
  - Gao B, Bataller R. Alcoholic liver disease: pathogenesis and new therapeutic targets. *Gastroenterology* 2011; 141:1572–1585.
  - Orman ES, Odena G, Bataller R. Alcoholic liver disease: pathogenesis, management, and novel targets for therapy. *J Gastroenterol Hepatol* 2013;28:77–84.
  - WHOMoSA Unit. Global status report on alcohol and health, 2018. World Health Organization, 2018.
  - Bataller R, Gao B. Liver fibrosis in alcoholic liver disease. *Semin Liver Dis* 2015;35:146–156.
  - Prado V, Caballería J, Vargas V, et al. Alcoholic hepatitis: how far are we and where are we going? *Ann Hepatol* 2016;15:463–473.
  - Louvet A, Mathurin P. Alcoholic liver disease: mechanisms of injury and targeted treatment. *Nature Reviews Gastroenterology & Hepatology* 2015;12:231.
  - World Health Organization. Ageing 2020.
  - Hayflick L. The future of ageing. *Nature* 2000; 408:267–269.
  - Blazer DG, Wu L-T. The epidemiology of at-risk and binge drinking among middle-aged and elderly community adults: National Survey on Drug Use and Health. *Am J Psychiatry* 2009;166:1162–1169.
  - Seitz HK, Stickel F. Alcoholic liver disease in the elderly. *Clinics in Geriatric Medicine* 2007;23:905–921.
  - Kim H, Kisseleva T, Brenner DA. Aging and liver disease. *Current Opinion in Gastroenterology* 2015;31:184.
  - Stahl EC, Haschak MJ, Popovic B, et al. Macrophages in the aging liver and age-related liver disease. *Frontiers in Immunology* 2018;9:2795.
  - Ren R, He Y, Ding D, et al. Aging exaggerates acute-on-chronic alcohol-induced liver injury in mice and humans by inhibiting neutrophilic sirtuin 1-C/EBP $\alpha$ -miRNA-223 axis. *Hepatology* 2022;75:646–660.
  - Meier P, Seitz HK. Age, alcohol metabolism and liver disease. *Current Opinion in Clinical Nutrition & Metabolic Care* 2008;11:21–26.
  - Timchenko NA. Aging and liver regeneration. *Trends Endocrinol Metab* 2009;20:171–176.
  - Cursio R, Colosetti P, Codogno P, et al. The role of autophagy in liver diseases: mechanisms and potential therapeutic targets. *BioMed Research International* 2015;2015.
  - Fernando R, Castro JP, Flore T, et al. Age-related maintenance of the autophagy-lysosomal system is dependent on skeletal muscle type. *Oxidative Medicine and Cellular Longevity* 2020:2020.
  - Liang W, Moyzis AG, Lampert MA, et al. Aging is associated with a decline in Atg9b-mediated autophagosome formation and appearance of enlarged mitochondria in the heart. *Aging Cell* 2020;19:e13187.
  - Dolganiuc A, Thomes PG, Ding WX, et al. Autophagy in alcohol-induced liver diseases. *Alcoholism Clin Exp Res* 2012;36:1301–1308.
  - Wang L, Khambu B, Zhang H, et al. Autophagy in alcoholic liver disease, self-eating triggered by drinking. *Clinics and Research in Hepatology and Gastroenterology* 2015;39:S2–S6.
  - Williams JA, Ding WX. Role of autophagy in alcohol and drug-induced liver injury. *Food and Chemical Toxicology* 2020:136.
  - Barbosa MC, Grosso RA, Fader CM. Hallmarks of aging: an autophagic perspective. *Frontiers in Endocrinology* 2019:790.
  - Martinez-Lopez N, Athonvarangkul D, Singh R. Autophagy and aging. *Longevity Genes* 2015:73–87.
  - Cuervo AM, Dice JF. Age-related decline in chaperone-mediated autophagy. *J Biol Chem* 2000; 275:31505–31513.
  - Singh R, Kaushik S, Wang Y, et al. Autophagy regulates lipid metabolism. *Nature* 2009;458:1131–1135.
  - Cuervo AM, Bergamini E, Brunk UT, et al. Autophagy and aging: the importance of maintaining "clean" cells. *Autophagy* 2005;1:131–140.
  - Schneider JL, Suh Y, Cuervo AM. Deficient chaperone-mediated autophagy in liver leads to metabolic dysregulation. *Cell Metabolism* 2014;20:417–432.
  - Schneider JL, Villarroja J, Diaz-Carretero A, et al. Loss of hepatic chaperone-mediated autophagy accelerates proteostasis failure in aging. *Aging Cell* 2015; 14:249–264.
  - Zhang C, Cuervo AM. Restoration of chaperone-mediated autophagy in aging liver improves cellular maintenance and hepatic function. *Nature Medicine* 2008;14:959–965.
  - Chao X, Wang S, Zhao K, et al. Impaired TFEB-mediated lysosome biogenesis and autophagy promote chronic ethanol-induced liver injury and steatosis in mice. *Gastroenterology* 2018;155:865–879 e12.
  - Thomes PG, Trambly CS, Fox HS, et al. Acute and chronic ethanol administration differentially modulate hepatic autophagy and transcription factor EB. *Alcohol Clin Exp Res* 2015;39:2354–2363.
  - Ma X, Chen A, Melo L, et al. Loss of hepatic DRP1 exacerbates alcoholic hepatitis by inducing megamitochondria and mitochondrial maladaptation. *Hepatology* 2023;77:159–175.
  - Bjorkoy G, Lamark T, Brech A, et al. p62/SQSTM1 forms protein aggregates degraded by autophagy and has a protective effect on huntingtin-induced cell death. *J Cell Biol* 2005;171:603–614.
  - Lahiri P, Schmidt V, Smole C, et al. p62/Sequestosome-1 is indispensable for maturation and stabilization of Mallory–Denk bodies. *PLoS One* 2016;11:e0161083.
  - Stumptner C, Fuchsichler A, Heid H, et al. Mallory body: a disease-associated type of sequestosome. *Hepatology* 2002;35:1053–1062.
  - Manley S, Williams JA, Ding WX. Role of p62/SQSTM1 in liver physiology and pathogenesis. *Exp Biol Med (Maywood)* 2013;238:525–538.

42. Moscat J, Diaz-Meco MT. p62 at the crossroads of autophagy, apoptosis, and cancer. *Cell* 2009;137:1001–1004.
43. Sanchez-Martin P, Saito T, Komatsu M. p62/SQSTM1: 'jack of all trades' in health and cancer. *FEBS Journal* 2019;286:8–23.
44. Qian H, Chao X, Williams J, et al. Autophagy in liver diseases: a review. *Mol Aspects Med* 2021:100973.
45. Kang L, Chen X, Sebastian BM, et al. Chronic ethanol and triglyceride turnover in white adipose tissue in rats: inhibition of the anti-lipolytic action of insulin after chronic ethanol contributes to increased triglyceride degradation. *J Biol Chem* 2007;282:28465–28473.
46. Zhong W, Zhao Y, Tang Y, et al. Chronic alcohol exposure stimulates adipose tissue lipolysis in mice: role of reverse triglyceride transport in the pathogenesis of alcoholic steatosis. *Am J Pathol* 2012;180:998–1007.
47. Li Y, Chao X, Wang S, et al. Role of mechanistic target of rapamycin and autophagy in alcohol-induced adipose atrophy and liver injury. *Am J Pathol* 2020;190:158–175.
48. Shen H, Jiang L, Lin JD, et al. Brown fat activation mitigates alcohol-induced liver steatosis and injury in mice. *J Clin Invest* 2019;129:2305–2317.
49. Fan MJ, Wang YM, Jin LH, et al. Bile acid-mediated activation of brown fat protects from alcohol-induced steatosis and liver injury in mice. *Cell Mol Gastroenterol Hepatol* 2022;13:809–826.
50. Rodriguez A, Duran A, Selloum M, et al. Mature-onset obesity and insulin resistance in mice deficient in the signaling adapter p62. *Cell Metabolism* 2006;3:211–222.
51. Muller TD, Lee SJ, Jastroch M, et al. p62 links beta-adrenergic input to mitochondrial function and thermogenesis. *J Clin Invest* 2013;123:469–478.
52. Fischer K, Fenzl A, Liu DX, et al. The scaffold protein p62 regulates adaptive thermogenesis through ATF2 nuclear target activation. *Nature Communications* 2020:11.
53. Bitto A, Lerner CA, Nacarelli T, et al. p62/SQSTM1 at the interface of aging, autophagy, and disease. *Age* 2014;36:1123–1137.
54. Kwon J, Han E, Bui CB, et al. Assurance of mitochondrial integrity and mammalian longevity by the p62-Keap1-Nrf2-Nqo1 cascade. *Embo Reports* 2012;13:150–156.
55. Komatsu M. p62 bodies: phase separation, NRF2 activation, and selective autophagic degradation. *lubmb Life* 2022;74:1200–1208.
56. Fu A, Cohen-Kaplan V, Avni N, et al. p62-containing, proteolytically active nuclear condensates, increase the efficiency of the ubiquitin-proteasome system. *Proc Natl Acad Sci U S A* 2021:118.
57. Prusty D, Park BH, Davis KE, et al. Activation of MEK/ERK signaling promotes adipogenesis by enhancing peroxisome proliferator-activated receptor gamma (PPAR gamma) and C/EBP alpha gene expression during the differentiation of 3T3-L1 preadipocytes. *J Biol Chem* 2002;277:46226–46232.
58. Stralfors P, Belfrage P. Phosphorylation of hormone-sensitive lipase by cyclic AMP-dependent protein kinase. *J Biol Chem* 1983;258:15146–15152.
59. Asterholm IW, Tao C, Morley TS, et al. Adipocyte inflammation is essential for healthy adipose tissue expansion and remodeling. *Cell Metabolism* 2014;20:103–118.
60. Murano I, Barbatelli G, Parisani V, et al. Dead adipocytes, detected as crown-like structures, are prevalent in visceral fat depots of genetically obese mice. *J Lipid Res* 2008;49:1562–1568.
61. Kajimura S, Spiegelman BM, Seale P. Brown and beige fat: physiological roles beyond heat generation. *Cell Metabolism* 2015;22:546–559.
62. Seale P, Bjork B, Yang WL, et al. PRDM16 controls a brown fat/skeletal muscle switch. *Nature* 2008;454:961–U27.
63. de Jesus LA, Carvalho SD, Ribeiro MO, et al. The type 2 iodothyronine deiodinase is essential for adaptive thermogenesis in brown adipose tissue. *J Clin Invest* 2001;108:1379–1385.
64. Barneda D, Planas-Iglesias J, Gaspar ML, et al. The brown adipocyte protein CIDEA promotes lipid droplet fusion via a phosphatidic acid-binding amphipathic helix. *Elife* 2015;4.
65. Reitman ML. FGF21: a missing link in the biology of fasting. *Cell Metabolism* 2007;5:405–407.
66. Kliewer SA, Mangelsdorf DJ. A dozen years of discovery: insights into the physiology and pharmacology of FGF21. *Cell Metabolism* 2019;29:246–253.
67. Liu YL, Zhao CQ, Xiao J, et al. Fibroblast growth factor 21 deficiency exacerbates chronic alcohol-induced hepatic steatosis and injury. *Sci Rep-Uk* 2016;6.
68. Coelho M, Oliveira T, Fernandes R. Biochemistry of adipose tissue: an endocrine organ. *Archives of Medical Science* 2013;9:191.
69. Kim IH, Kisseleva T, Brenner DA. Aging and liver disease. *Curr Opin Gastroenterol* 2015;31:184–191.
70. Fan X, Huang T, Tong Y, et al. p62 works as a hub modulation in the ageing process. *Ageing Res Rev* 2022;73:101538.
71. Ramesh Babu J, Lamar Seibenhener M, Peng J, et al. Genetic inactivation of p62 leads to accumulation of hyperphosphorylated tau and neurodegeneration. *J Neurochemistry* 2008;106:107–120.
72. Wang L, Ebrahimi KB, Chyn M, et al. Biology of p62/sequestosome-1 in age-related macular degeneration (AMD). *Retinal Degenerative Diseases* 2016:17–22.
73. Du Y, Wooten MC, Gearing M, et al. Age-associated oxidative damage to the p62 promoter: implications for Alzheimer disease. *Free Radic Biol Med* 2009;46:492–501.
74. Sasaki M, Miyakoshi M, Sato Y, et al. A possible involvement of p62/sequestosome-1 in the process of biliary epithelial autophagy and senescence in primary biliary cirrhosis. *Liver Int* 2012;32:487–499.
75. Li Y, Ding WX. Adipose tissue autophagy and homeostasis in alcohol-induced liver injury. *Liver Res* 2017;1:54–62.
76. McCullough RL, McMullen MR, Poulsen KL, et al. Anaphylatoxin receptors C3aR and C5aR1 are important factors that influence the impact of ethanol on the adipose secretome. *Front Immunol* 2018;9.
77. Naveau S, Giraud V, Borotto E, et al. Excess weight risk factor for alcoholic liver disease. *Hepatology* 1997;25:108–111.



78. Parker R, Kim SJ, Im GY, et al. Obesity in acute alcoholic hepatitis increases morbidity and mortality. *EBioMedicine* 2019;45:511–518.
79. Zhao CQ, Liu YL, Xiao J, et al. FGF21 mediates alcohol-induced adipose tissue lipolysis by activation of systemic release of catecholamine in mice. *J Lipid Res* 2015; 56:1481–1491.
80. Cao WH, Daniel KW, Robidoux J, et al. p38 mitogen-activated protein kinase is the central regulator of cyclic AMP-dependent transcription of the brown fat uncoupling protein 1 gene. *Mol Cell Biol* 2004;24:3057–3067.
81. Zhang Y, Goldman S, Baerga R, et al. Adipose-specific deletion of autophagy-related gene 7 (atg7) in mice reveals a role in adipogenesis. *Proc Natl Acad Sci U S A* 2009;106:19860–19865.
82. Singh R, Xiang YQ, Wang YJ, et al. Autophagy regulates adipose mass and differentiation in mice. *J Clin Invest* 2009;119:3329–3339.
83. Yang H, Ni H-M, Guo F, et al. Sequestosome 1/p62 protein is associated with autophagic removal of excess hepatic endoplasmic reticulum in mice. *J Biol Chem* 2016;291:18663–18674.
84. Bertola A, Mathews S, Ki SH, et al. Mouse model of chronic and binge ethanol feeding (the NIAAA model). *Nat Protoc* 2013;8:627–637.
85. Williams JA, Ni HM, Ding Y, et al. Parkin regulates mitophagy and mitochondrial function to protect against alcohol-induced liver injury and steatosis in mice. *Am J Physiol Gastrointest Liver Physiol* 2015;309:G324–G340.
86. Chao X, Wang S, Hlobik M, et al. Loss of hepatic transcription factor EB attenuates alcohol-associated liver carcinogenesis. *Am J Pathol* 2021.
87. Wang F, Zhang Y, Shen J, et al. The ubiquitin E3 ligase TRIM21 promotes hepatocarcinogenesis by suppressing the p62-Keap1-Nrf2 antioxidant pathway. *Cell Mol Gastroenterol Hepatol* 2021;11:1369–1385.
88. Ni H-M, Boggess N, McGill MR, et al. Liver-specific loss of Atg5 causes persistent activation of Nrf2 and protects against acetaminophen-induced liver injury. *Toxicol Sci* 2012;127:438–450.

---

Received August 31, 2022. Accepted January 31, 2023.

#### Correspondence

Address correspondence to: Wen-Xing Ding, PhD, Department of Pharmacology, Toxicology and Therapeutics, University of Kansas Medical Center, MS 1018, 3901 Rainbow Boulevard, Kansas City, Kansas 66160. e-mail: wxding@kumc.edu.

#### CRedit Authorship Contributions

Hui Qian (Data curation: Lead; Formal analysis: Lead; Investigation: Lead; Methodology: Lead; Software: Lead; Writing – original draft: Lead; Writing – review & editing: Supporting)

Xiaojuan Chao (Data curation: Supporting; Investigation: Supporting; Methodology: Supporting)

Shaogui Wang (Data curation: Supporting; Investigation: Supporting; Methodology: Supporting)

Yuan Li (Data curation: Supporting; Investigation: Supporting; Methodology: Supporting)

Xiaoxiao Jiang (Data curation: Supporting; Methodology: Supporting)

Zhaoli Sun (Resources: Supporting)

Thomas Rüllicke (Resources: Supporting; Writing – review & editing: Supporting)

Kurt Zatloukal (Resources: Supporting)

Hong-Min Ni (Data curation: Supporting; Investigation: Supporting; Methodology: Supporting; Resources: Supporting; Writing – review & editing: Supporting)

Wen-Xing Ding (Conceptualization: Lead; Funding acquisition: Lead; Project administration: Lead; Supervision: Lead; Writing – original draft: Equal; Writing – review & editing: Lead)

#### Conflicts of interest

The authors disclose no conflicts.

#### Funding

Supported in part by the National Institutes of Health (NIH) funds R01 DK102142, R01 AG072895, and R37 AA020518 (WXD).